UNSATURATED SOIL PROPERTIES OF INTACT SAMPLES OF ANKARA CLAY

A THESIS SUBMITTED TO
THE GRADUATE SCHOOL OF NATURAL AND APPLIED SCIENCES
OF
MIDDLE EAST TECHNICAL UNIVERSITY

BY

MAHAM BASHARAT

IN PARTIAL FULFILLMENT OF THE REQUIREMENTS
FOR
THE DEGREE OF MASTER OF SCIENCE
IN
CIVIL ENGINEERING

JUNE 2024

Approval of the thesis:

UNSATURATED SOIL PROPERTIES OF INTACT SAMPLES OF ANKARA CLAY

submitted by **MAHAM BASHARAT** in partial fulfillment of the requirements for the degree of **Master of Science** i**n Civil Engineering, Middle East Technical University** by,

Prof. Dr. Naci Emre Altun
Dean, **Graduate School of Natural and Applied Sciences** _____

Prof. Dr. Erdem Canbay
Head of the Department, **Civil Engineering** _____

Assoc. Prof. Dr. Nabi Kartal Toker
Supervisor, **Civil Engineering, METU** _____

Examining Committee Members:

Prof. Dr. Erdal Çokça
Civil Engineering Dept., METU _____

Assoc. Prof. Dr. Nabi Kartal Toker
Civil Engineering Dept., METU _____

Assoc. Prof. Dr. Nejan Huvaj Sarıhan
Civil Engineering Dept., METU _____

Prof. Dr. Taha Taşkiran
Civil Engineering Dept., Ankara Yıldırım Beyazıt University _____

Prof. Dr. Bahadır Sadık Bakır
Civil Engineering Dept., METU _____

Date: 12.06.2024

I hereby declare that all information in this document has been obtained and presented in accordance with academic rules and ethical conduct. I also declare that, as required by these rules and conduct, I have fully cited and referenced all material and results that are not original to this work.

Name Last name : Maham Basharat

Signature :

ABSTRACT

UNSATURATED SOIL PROPERTIES OF INTACT SAMPLES OF ANKARA CLAY

Basharat, Maham
Master of Science, Civil Engineering
Supervisor: Assoc. Prof. Dr. Nabi Kartal Toker

June 2024, 108 pages

The city of Ankara is home to predominantly clays which are highly plastic, very stiff and fissured. Moreover, water table is encountered at a depth of 15m. This essentially means that the prevalent soil of Ankara is unsaturated clay. The behavior of unsaturated soils is quite different than that of saturated soils, mainly due to the influence of suction. For this reason, it is imperative that the behavior of Ankara soils be studied in detail under various modes of stress and suction loadings. This study investigates the unsaturated behavior of Ankara clay subject to various loadings at various degrees of saturation. Samples were collected from all over the region and tests were performed to determine their crucial properties as well as behavior. The results of the tests demonstrate the high values of suction Ankara clay can have even when fully saturated (~38 MPa). They also provide insight into the unexpectedly low increase in shear and compressive strength with a decrease in the degree of saturation. Finally, an attempt to model the behavior of Ankara clay using the Barcelona Basic Model (BBM) was carried out. Results of the calibration prove that BBM fails to accurately capture the brittle behavior of Ankara clay at high suctions.

Keywords: Unsaturated Clay, Undisturbed Sample, Stiff Clay, CW Testing

ÖZ

ANKARA KİLİNİN SAĞLAM ÖRNEKLERİNİN DOYMAMIŞ ÖZELLİKLERİ

Basharat, Maham
Yüksek Lisans, İnşaat Mühendisliği
Tez Yöneticisi: Doç. Dr. Nabi Kartal Toker

Haziran 2024, 108 sayfa

Ankara şehri ağırlıklı olarak yüksek derecede plastik, çok sert ve çatlaklı kil türlerine ev sahipliği yapmaktadır. Ayrıca 15 m derinlikte su tablasına rastlanmaktadır. Bu aslında Ankara'nın hakim toprağının doymamış kil olduğu anlamına gelir. Doygun olmayan zeminlerin davranışı, esas olarak emme etkisinden dolayı, doymuş zeminlerden oldukça farklıdır. Bu nedenle Ankara zeminlerinin çeşitli gerilme ve emme yükleri altındaki davranışının ayrıntılı olarak incelenmesi zorunludur. Bu çalışma, Ankara kilinin çeşitli doygunluk derecelerinde çeşitli yüklemelere maruz kalan doygun olmayan davranışını araştırmaktadır. Bölgenin her yerinden örnekler toplandı ve bunların önemli özelliklerinin yanı sıra davranışlarını belirlemek için testler yapıldı. Testlerin sonuçları, Ankara kilinin tamamen doygun durumda bile sahip olabileceği yüksek emme değerlerine (~38 MPa) işaret etmektedir. Ayrıca doygunluk derecesindeki azalmayla birlikte kesme ve basınç dayanımındaki beklenmedik derecede düşük artışa ilişkin bilgi sağlarlar. Son olarak Ankara kilinin davranışını Barselona Temel Modeli (BBM) kullanılarak modelleme girişimi gerçekleştirildi. Kalibrasyon sonuçları, BBM'nin Ankara kilinin yüksek emmelerdeki kırılgan davranışını doğru bir şekilde yakalayamadığını kanıtlıyor.

Anahtar Kelimeler: Doygun olmayan kil, Örselenmemiş numune, Katı kil, CW deney

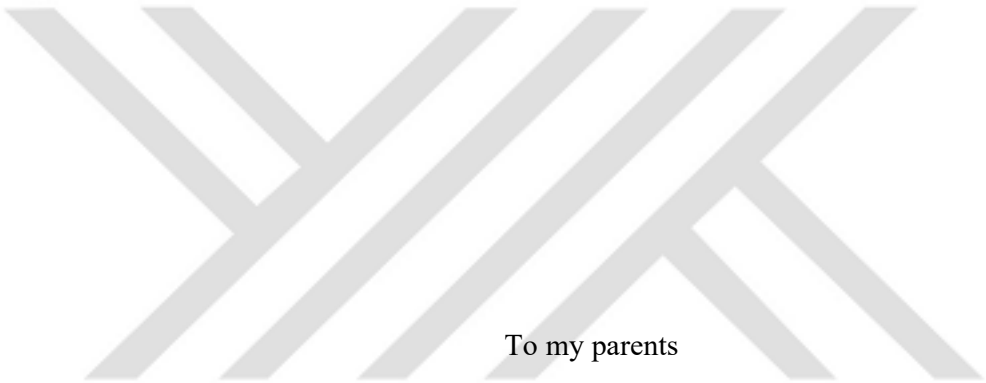

To my parents

ACKNOWLEDGMENTS

I would like to express my deepest gratitude to my supervisor, Assoc. Prof. Dr. Nabi Kartal Toker for his guidance, advice and his endless patience for my antics. I have learned a great deal from him and it was a privilege to have worked with him.

I would also like to extend my appreciation to the faculty and staff at Middle East Technical University for their support and guidance. Special thanks to Mr. Kamber Bilgen, laboratory assistant in the Soil Mechanics Lab, for always being a helping hand.

Many thanks to my friends and colleagues at METU. They made my time in Turkey enjoyable and memorable. Special thanks to Berkan for always being in the lab and helping me whenever something went wrong and also to Melih for always being there to guide me.

My deepest love and appreciation to my friends back home for always encouraging me and being proud of me. Maavra, Fatima and Zainab for being my rocks, through the good times and the bad times. Ajwat for being a dear friend and colleague.

Last, but certainly not the least, my endless love and thanks to my parents and sisters. Their love motivates me and keeps me going, no matter how difficult times get. I owe all my success to them.

TABLE OF CONTENTS

LIST OF TABLES

TABLES

LIST OF FIGURES

FIGURES

LIST OF ABBREVIATIONS

ABBREVIATIONS

SWRC	Soil Water Retention Curve
AEV	Air Entry Value
HAE	High Air Entry
PEG	Polyethylene Glycol
BBM	Barcelona Basic Model
MCC	Modified Cam Clay
ASTM	American Society for Testing and Materials
LL	Liquid Limit
PL	Plastic Limit
PI	Plasticity Index
AASHTO	American Association of State Highway and Transportation Officials
USCS	Unified Soil Classification System
METU	Middle East Technical University
FCT	Fall Cone Test
RH	Relative Humidity
CD	Consolidated Drained
UU	Unconsolidated Undrained
ATS	Apparent Tensile Strength

LIST OF SYMBOLS

u_a	Air Pressure
u_w	Water Pressure
κ	Mean Curvature
σ_{st}	Surface Tension
φ	Contact Angle
T_s	Surface Tension
θ	Volumetric Water Content
θ_{sat}	Saturated Volumetric Water Content
θ_{res}	Residual Volumetric Water Content
ψ	Suction
ψ_{res}	Residual Suction
ψ_{aev}	Air Entry Value of Suction
λ	Pore Size Distribution Index
p_c	Reference Stress
p_0^*	Pre-consolidation Pressure for Saturated Condition
$\lambda(0)$	Slope of Virgin Compression Line
M	Slope of Critical State Line
c''	Apparent Cohesion
γ_w	Density Of Water
Cc	Compression Index
Cs	Swelling Index
C_v	Coefficient Of Consolidation
t_{100}	Time Taken For Primary Consolidation
σ_3	Minor Stress
σ_1	Major Stress
σ_{dev}	Deviator Stress
σ_{mean}	Mean Stress
$\lambda(0)$	Cc for the Saturated State Along Virgin Loading
κ	Compressibility Coefficient Along Unloading-Reloading Stress Path
r	Minimum Value Of The Cc For High Suctions
β	Parameter Controlling the Rate of Increase of Stiffness (Virgin States) with Suction
k	Parameter Controlling the Increase in Cohesion with Suction,

CHAPTER 1

INTRODUCTION

1.1 Motivation

Unsaturated soil mechanics aims to bridge the gap between conventional soil mechanics and actual soil behavior. This is largely due to the fact that conventional soil mechanics relies on some broad assumptions such as the fact that it assumes soil to be in a saturated state at all times. This leads to conservative design which is thought to be safer but is costly and inefficient. However, that is not always the main risk, especially in arid climates if unsaturated properties are mistaken for saturated ones or with expansive and collapsible soils. Furthermore, this conservative design is often costly and inefficient.

Unsaturated soil mechanics, as is obvious by its name, forgoes this assumption and accounts for the variations in the degree of saturation and the strength that it lends to the soil. This, in turn, allows researchers to model the strength of the soils in a more comprehensive framework. It also allows them to measure—and even predict—the change in the strength with a change in the moisture content caused by precipitation patterns throughout the year.

1.2 Problem Statement

In the past, several studies have been carried out on unsaturated soils in order to gain better insight into their behavior and strength characteristics. Particularly, recent decades have seen rapid advancements in both constitutive modeling and laboratory behavior of unsaturated soils. However, studies typically tend to rely on reconstituted

samples of soil, especially for studies focusing on clayey soils. These samples are reconstituted from slurry and then isotropically consolidated in laboratory settings at low pressures.

Nevertheless, this approach presents a few limitations. Firstly, the reconstitution procedure is adopted because it is thought to erase the stress history of the specimens. However, sometimes it can lead to complicated stress histories which alter the subsequent behavior of the soil or soil fabric (Ahmadi Naghadeh, 2016). Furthermore, specimens that are normally consolidated in the lab at low pressures cannot accurately mirror the behavior experienced in the field. This is because, in the field, unsaturated soils are typically heavily overconsolidated due to desiccation-induced suction stress and their pre-consolidation pressure is also much higher than what can be achieved in the lab.

The pre-consolidation pressure, over-consolidation ratio and stress history have a considerable impact on the behavior of the soil. Therefore, for accurate predictions, it is always recommended to extract undisturbed samples from the field and test the behavior of those directly.

This study aims to take a step in bridging this gap, particularly for Ankara clay, by studying its in-situ unsaturated soil properties. Ankara clay is reddish-brown, expansive and unsaturated clay found in the greater Ankara region. Currently, the literature available on this particular soil focuses heavily on its swelling characteristics as well as its potential as a clay liner.

There have only been a few investigations into its unsaturated soil properties. However, all of those studies make use of reconstituted samples which are subject to the problems described above. Additionally, the results of these reconstituted samples cannot be used in local practice because, as mentioned previously, they do not accurately capture the behavior of soil in the field. This is because, in its in-stu state, Ankara clay typically has a smaller void ratio and also swells less when exposed to water. However, smaller void ratios can also mean higher suction within

the soil. Therefore, it was deemed crucial to investigate the behavior of Ankara clay in its in-situ state.

Furthermore, as mentioned previously, recent decades have seen rapid advancements in laboratory testing of unsaturated soils. New techniques have been developed which capture the unsaturated behavior of soils in a more rapid and practical manner. They make use of less sophisticated equipment and also deliver results a lot quicker. However, these techniques have also been developed and validated using reconstituted samples. Hence, there is a need to test these methods using intact samples in order to validate their applicability for soils experiencing high suctions.

1.3 Scope

This study aims to investigate the behavior of unsaturated Ankara clay specimens in their undisturbed form. Firstly, samples were extracted from two sites in Ankara. Their index properties were discerned through basic tests and soil type characterization was carried out. A comprehensive laboratory testing program was developed to determine the hydraulic and mechanical properties of the specimen. Soil Water Retention Curve (SWRC) and shrinkage curve were also developed.

In Chapter 2, a comprehensive literature review is presented, detailing the research that has been conducted on unsaturated soil behavior. Chapter 3 provides details regarding the basic properties and soil type classification of the specimens. Chapter 4 concerns the hydraulic properties of the soil and the experiments conducted to determine them. Chapter 5 covers the mechanical properties of the specimens and relevant experiments. Chapter 6 combines the results of all experiments. Finally, chapter 7 provides conclusions and recommendations for future studies.

CHAPTER 2

LITERATURE REVIEW

2.1 Unsaturated Soil Properties

Soil is a three-phase porous medium i.e. it consists of solid particles with pores in between. These pores can contain water, air or a combination of both. The retention of water in these pores can be attributed to either capillary or adsorption mechanisms. Adsorption is the process by which water becomes attached to the surface of soil particles due to intermolecular forces. Capillarity is the process through which water is held in the pores of the soil due to the interfacial tension between water and air.

Water is able to travel within the pores of the soil. However, the transport of water through the pores is dependent on various factors such as pore size, particle geometry, contact angle of water and soil as well as the spatial change in potential. Soil water potential is defined as "*the work needed per quantity of pore water to transfer (reversibly and isothermally) an infinitesimal quantity of water from a pool of pure water at reference elevation and external air pressure to soil pores*" (Aitchison, 1965).

There are several components of total soil water potential such as gravitational, pressure, matric and osmotic (Fredlund et al., 2012). Gravitational potential arises from the force of gravity and pressure potential can be attributed to external gas forces in the atmosphere. Details regarding matric and osmotic potential can be found in the next section.

2.1.1 Matric and Osmotic Suction

As discussed in the previous sections, matric and osmotic potentials (i.e. negative pressures) influence the transport of water through soil. This, in turn, influences the behavior of soil in an unsaturated state. Suction is the term given to denote negative pressure in unsaturated soils.

Osmotic suction is derived from the presence of dissolved ions in water. These ions influence the vapor pressure in the pores which, in turn, influences the relative humidity which leads to a change in the soil suction level. Mathematically, it can be expressed as:

$$h_s = \frac{n}{V}.R.T \qquad \text{(Eq 2.1)}$$

where n/V is the total ion concentration (molar), R is the universal gas constant and T is the absolute temperature in Kelvins. In most geotechnical problems, osmotic suction is not taken into account as significant changes do not occur in its levels.

Matric suction refers to the negative pressure experienced by soil water due to the capillary phenomenon. Mathematically, it is expressed as the difference between air and water pressure (u_a-u_w). It can also be expressed using the Young-Laplace equation:

$$u_a - u_w = 2\kappa\sigma_{st} \qquad \text{(Eq 2.2)}$$

where κ is the mean curvature and σ_{st} is the surface tension at the water-air interface.

Physically, the phenomena of matric suction or capillarity can be explained by using the example of a thin tube inserted in a beaker of water (see Figure 2.1). Water rises up the tube and forms a meniscus. This is because of adhesive and cohesive forces.

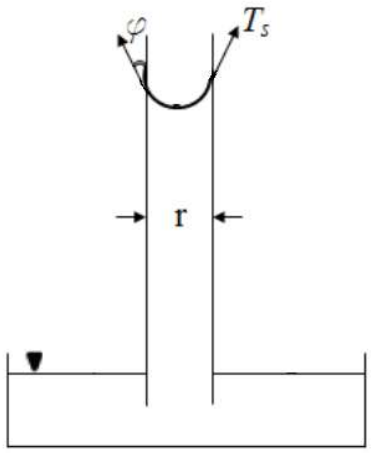

Figure 2.1. Capillary rise phenomenon

Adhesive forces are present between the water molecules and the edge of the tube, forming a contact angle (φ). Cohesive forces are present between water molecules. Furthermore, a water molecule inside the water experiences equal amounts of intermolecular forces from each side. However, at the edge of the air-water interface, water experiences more force from the inwards side due to the absence of water molecules on the outside. This phenomenon results in a curved surface under tension (T_s). The adhesion forces are balanced by the surface tension and the radius of curvature of the meniscus.

2.1.2 Soil Water Retention Curve

The soil water retention curve (SWRC) defines the relationship between the amount of moisture in the soil and the suction. The amount of moisture in the soil can be related to the degree of saturation, volumetric water content or gravimetric water content. Typically, soil is fully saturated up to a threshold value of suction, after which it begins to lose moisture. This is known as the air-entry value (AEV) of suction. Once the AEV is surpassed, soil becomes partially saturated and begins to lose moisture as suction increases. This range of values of suction is known as the transition zone, bulk drainage regime or funicular regime. This trend continues until,

finally, the graph tapers off and moisture content becomes relatively constant at high values of suction. This is called 'residual moisture content' or 'pendular regime' (see Figure 2.2).

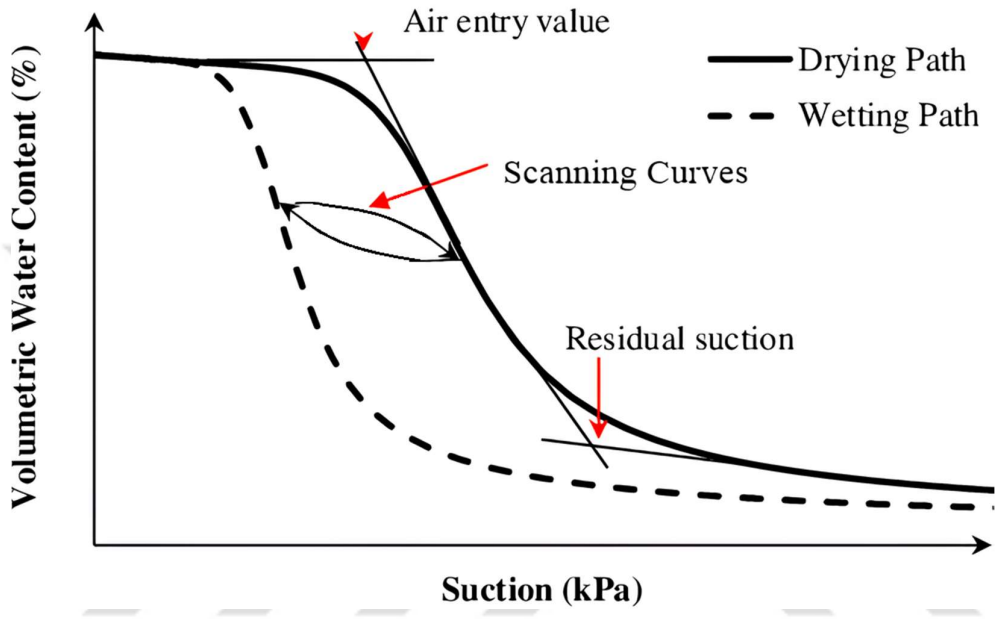

Figure 2.2. A typical soil water retention curve (Shwan, 2017)

It is also important to note here that the SWRC is hysteretic in nature, as displayed in Figure 2.2. This essentially means that during the drying and wetting regime of the soil, it may have different values of suction at the same moisture content (Fredlund et al., 2012). When a fully dry specimen is wetted for retention curve measurement, it gives us the primary 'wetting curve.' Conversely, a saturated specimen dries on the main 'drying curve.' However, if the soil specimen is wetted or dried from an intermediate point, it results in scanning curves, which span the intermediary zone between the main wetting and drying curves.

SWRCs can be determined from experimental techniques (see section 2.2.2 for details) or from empirical equations. These empirical equations can be attributed to various researchers who, throughout the past decades, have attempted to fit mathematical equations to experimental data. Table 2.1 highlights some of the most commonly used equations.

Table 2.1 Most commonly used SWRC equations

Reference	Equation
(Brooks & Corey, 1965)	$\theta = \theta_{res} + (\theta_{sat} - \theta_{res})(\frac{\psi}{\psi_{aev}})^{-\lambda}$
(Van Genuchten, 1980)	$\theta = \theta_{res} + \frac{\theta_{sat} - \theta_{res}}{(1 + (\frac{\psi}{\psi_{aev}})^{n})^{m}}$
(D. G. Fredlund & Xing, 1994)	$\frac{\theta}{\theta_{sat}} = (1 - \frac{\ln\left(1 + \frac{\psi}{\psi_{res}}\right)}{\ln\left(1 + \frac{(10^{6}\ kPa)}{\psi_{res}}\right)}) * (\ln\left(e + \left(\frac{\psi}{a}\right)^{n}\right))^{-m}$

where, θ is the volumetric water content, θ_{sat} is the saturated volumetric water content (or porosity), θ_{res} is the residual volumetric water content, ψ is the suction, ψ_{res} is the suction corresponding to the residual water content, ψ_{aev} is the air-entry value of the suction, λ is the pore size distribution index and a, n, m are fitting parameters.

2.2 Experimental Testing of Unsaturated Soils

Throughout the past decades of studies in this field, advances have been made in experimental techniques and procedures that aim to capture and determine the properties and behavior of unsaturated soils. This includes techniques to measure the SWRC, hydraulic conductivity and shear strength.

2.2.1 Suction Control Techniques

There exist several methods to control or impose a certain level of suction on a soil specimen. This will, in turn, cause the moisture content of the specimen to change. The suction imposed can be either total or matric suction.

Total Suction

Total suction can be determined using the Kelvin's equation which is as follows:

$$\psi = \frac{-\gamma_w RT}{(MW)_w} \ln(RH) \quad \text{(Eq 2.3)}$$

where ψ is the suction in kPa, γ_w is the density of water, (MW)w is the molar weight of water (18.016 g/mol), R is the ideal gas constant (8.314 J/mol), T is the temperature in Kelvin and RH is the relative humidity in decimal form.

Total suction can be imposed on a soil specimen by equilibrating it with a salt solution's osmotic suction without allowing the salt ions to move into the soil pores (Blatz et al., 2009). This can typically be achieved by enclosing the specimen in an air chamber with the salt solution. The specimen is elevated using a stand so as to avoid contact and the chamber is sealed in order to ensure humidity equilibrium. The relative humidity of the chamber due to the salt solution equilibriates with that of the soil and, consequently, imposes suction on it.

Alternatively, the salt solution can also be connected to the soil water through a semipermeable membrane which allows the water molecules to pass through it but not the salt molecules. However, these methods have extremely high equilibration times (up to several months) and are also very susceptible to temperature changes (Blatz et al., 2009). Small changes in temperature can lead to drastic changes in suction levels, thus introducing errors in the measurements.

Another method of total suction imposition is what is referred to as the divided airflow setup. It is done by connecting the soil specimen to two chambers, one with completely dry air (0% humidity) and one with totally humid air (100% humidity). The flow of air from both chambers is independently controlled which allows a certain level of humidity (adjustable by the operator) to flow to the specimen. This, in turn, imposes suction on the soil.

Matric Suction

Matric suction can be imposed by several methods. The first one is the hanging column setup, sometimes also known as the negative column setup (Vanapalli et al., 2009). This setup consists of a soil specimen on top of a high air entry (HAE) ceramic that restricts the flow of air into the specimen and only allows water. The HAE is, in turn, connected to a water column with an adjustable height difference from a water surface open to the atmosphere. Changing the height of the water column imposes suction on the soil due to a change in gravitational potential. However, suctions imposed by this method are very low (typically less than 90kPa), as limited by cavitation and physical dimensions.

Another method of inducing matric suction is the centrifuge. A soil specimen is placed inside a centrifuge and spun at excessively high speeds. This induces extra gravity which, subsequently, induces matric suction on a specimen that is open to gravity drainage (Caicedo & Thorel, 2014).

Axis translation is also another technique used to impose matric suction on a soil specimen. In this technique, a soil specimen is placed in an enclosed chamber with an HAE ceramic at the bottom of it. Air pressure is introduced in the chamber from the top. The HAE ceramic at the bottom is connected to the water pressure inlet. The air pressure is always kept greater than the water pressure and, hence, matric suction is introduced (Lu, 2019).

However, this technique has certain experimental difficulties associated with it. Firstly, the high air pressure causes air to dissolve. Dissolved air can diffuse through the ceramic and come out of the solution on the low-pressure side, causing air bubbles to accumulate beneath the HAE ceramic (Khallili et al., 2022). This disconnects the specimen from the water pressure. To overcome this, the procedure of flushing the air bubbles at regular intervals is suggested in the literature (Vanapalli et al., 2009). This can be done either manually by using a syringe or automatically by using a pump (Kenanoğlu, 2023).

Another difficulty associated with this technique is the estimation of the equilibriation time (Oliveira & Marinho, 2008). To overcome this, (Kenanoğlu, 2023) developed a setup where the water inlet pipes are inserted in a beaker so as to keep the water pressure at 0 kPa gage pressure. The beaker is then placed on a mass balance and loss in mass is recorded every day. Either before or in parallel with starting the test, the rate of evaporation is measured in the place where the test is to be conducted. Hence, when the daily loss in mass became equal to the rate of evaporation calculated prior to the test, equilibrium was achieved. However, this technique is also subject to errors as a pre-calibrated rate of evaporation can vary according to temperature and other climatic factors.

2.2.2 Suction Measurement Techniques

An alternative to suction control is suction measurement. The aim is to measure the suction level in any soil specimen without attempting to control or change it. The difference is akin to the distinction between pore pressure control in a CD triaxial and pore pressure measurement in a CU triaxial test. These techniques are particularly helpful during in-situ tests.

Osmotic Suction

Osmotic suction can be measured by extracting the pore water by what is commonly known as the ‘squeezing technique’ (Peroni & Tarantino, 2005; ASTM D4542-22) and measuring its suction. The electrical conductivity of the extracted pore water is measured. This has a linear relationship with osmotic suction when both parameters are plotted on a logarithmic scale. This method can measure suctions up to 35 Mpa.

Total Suction

Total suction can be measured using a psychrometer, which is a device used to measure humidity. Psychrometers can rely on thermisters or thermocouples. They can also be directly inserted into soil to measure the in-situ suction. Their equilibration time tends to vary from a few hours to several days and they can

measure suctions up to 7.5 MPa. However, readings taken at lower values of suction are more susceptible to error by temperature fluctuation (Bulut & Leong, 2008).

Another method of total suction measurement is the chilled mirror hygrometer technique. This technique makes use of the chilled mirror dew point technique in an enclosed chamber. The soil specimen is placed in the chamber and it is sealed off. Also present in the chamber is a metal mirror which is cooled to the point where it attracts condensation. Light is then shined on the mirror using a laser from where it is reflected onto a sensor. The sensor detects the intensity of the reflected light which is used to deduce the amount of condensation on the mirror which, in turn, is indicative of the relative humidity in the enclosed chamber. The relative humidity then allows us to infer the suction in the soil. However, (Leong et al., 2003) evaluated the accuracy of this device and discovered that it overrepresented the total suction in soils.

Total suction can also be measured by equilibrating soil specimens in an enclosed chamber with filter paper which has a known retention curve. The two are placed such that they are not in contact with one another. This setup can take up to a few weeks to equilibrate. However, it has been discovered to have large error margins which is why it is not preferred (Bulut & Leong, 2008).

Matric Suction

Matric suction can be measured using various devices and methods. A conventional suction measurement device for the field is the tensiometer which has a water reservoir at the top and an HAE ceramic at the bottom of a tube that can be up to a few metres long. The porous tip is inserted into the soil where it equilibrates rather quickly with the soil and gives a suction reading. However, this device can measure suction only up to about 90 kPa.

Osmotic tensiometers are also used where a semi-permeable membrane is placed with soil specimen on one side and a solution of known suction that contains water and polyethylene-glycol (PEG). A pressure measurement device is attached to the

PEG solution and the reading it displays is the difference of suction in the PEG and the soil, allowing the user to determine the suction of the specimen.

In recent decades, high-capacity tensiometers have been developed with a range of up to 1.5-2.5 MPa (Ridley & Burland, 1993; Tarantino & Mongiovì, 2001; Delage et al., 2008). (Mendes et al., 2019)used a special nanoporous glass instead of porous ceramic and was able to measure matric suction up to 7.3 MPa.

2.2.3 Measurement of Soil Water Retention Curve

SWRC is commonly measured by extracting data points that correspond to moisture content at various suction levels. Researchers typically extract several data points over a wide range of suction and then attempt to fit one of the empirical equations devised for SWRCs to this data.

Due to the wide range of suction on the abscissa of a retention curve, a combination of two or more methods is often needed in order to extract all data points for the whole curve. For very low suctions (<90 kPa), the hanging column technique is used as discussed in section 2.2.1.

For mid-range values, a number of techniques can be applied such as axis translation (see section 2.2.1). This is typically done using pressure plate extractors wherein air pressure is applied to the specimen from the top. Water pressure is kept constant and equal to atmospheric pressure and it is introduced from the bottom. The specimens equilibrate under a given value of suction and water content can then be measured. These can typically measure values of suction up to 1500 kPa.

For high values of suction, the vapor equilibrium technique is used which can measure suction values up to 300 MPa (Gao & Sun, 2017). This technique is employed because it does not involve the application of large amounts of air pressure like in axis translation which can be a logistical and physical hurdle in laboratory settings. It also involves simple apparatus and procedures. However, its only downside is the large equilibriation times which can be upwards of several months.

In this way, a retention curve for a soil specimen can be obtained with several data points. This allows for more accurate calibration with numerical equations. It also enables researchers to more accurately capture the drying and wetting behavior of soil.

Alternative ways that can obtain the SWRC as a continuous curve also exist. (Sjoblom, 2000) and (Toker et al., 2004) extracted continuous data measurements for SWRC by the evaporation method. However, this method proved to have limited applicability as they could only obtain drying curves. Furthermore, this was not applicable for expansive clays as they tend to develop cracks and gaps during drying.

Other researchers combined a syringe pump with axis translation for continuous SWRC measurement (Lu et al., 2006; Mun & McCartney, 2015). There have also been studies correlating Mercury Intrusion Porosimeter (MIP) results to a continuous SWRC (Leech et al., 2006).

2.2.4 Constant Water Content Tests on Unsaturated Soils

When testing soil specimens under unsaturated conditions, researchers either control or measure the suction using one of the techniques described above. The tests in which suction is controlled at a certain value are called constant suction tests whereas when suction is measured, it is known as a constant water test. This is because, in such tests, air drainage is permitted (to allow compression) but water drainage is restricted (Fredlund et al., 2012). Water content is measured before, during and after the test and suction is inferred from SWRC data.

Constant water tests are preferred because the equilibration time is less than that of constant suction tests (Riad & Zhang, 2022). Furthermore, constant suction tests require sophisticated equipment which may not be readily available in most laboratory settings. However, constant water tests can be conducted on conventional setups with minor modifications (Ahmadi Naghadeh et al., 2013).

Furthermore, it has been discovered that at high suctions, suction is independent of the void ratio (Chen et al., 2021). Therefore, if constant water content tests are conducted at high suctions, when the void ratio changes during shear or compression, the degree of saturation might change but suction can be assumed constant. In this way, constant water content tests at high values of suction may serve as constant suction tests as well.

Over the years, researchers have conducted a wide variety of constant water content tests such as triaxial (A. M. Marinho et al., 2016; Li & Zhang, 2015; Mendes & Toll, 2016) and oedometer tests (Wijaya & Leong, 2016; Zhang et al., 2016). The results of these tests have also successfully been used for inferring soil properties and constitutive modeling (Riad & Zhang, 2022; Chiu & Ng, 2003; Ng et al., 2020). Therefore, constant water content tests are widely accepted and often practiced.

2.3 Evaporation Test

'Soil fabric' is a term used to describe the arrangement of soil particles, pores and pore fluids in a sample (Mitchell, 1976). The influence of soil fabric on the hydromechanical behavior of the soil has been studied extensively and there is sufficient evidence to prove that soil fabric does affect the hydromechanical behavior of soil, even in unsaturated states (Kochmanová & Tanaka, 2011; Nowamooz & Masrouri, 2010).

When considering the soil fabric, two types of soil water are considered: the water in macro (intra-aggregate) and micro (inter-aggregate) pores. The critical moisture content is a parameter used to differentiate between the water held in micro and macropores of the soil. This is an important property to determine as water held in the macropores due to capillary action is subject to mechanical actions (Romero et al., 1999). On the other hand, water held in micropores due to adsorption is essentially immobile and, therefore, is not affected by mechanical action.

There exist a multitude of methods to determine the critical moisture content of a soil. However, several of these methods are difficult to implement on expansive soils due to changing void ratios (Alonso et al., 2010; Lu, 2020). This is because all methods of evaporation test involve drying of the soil which changes its surface area and void ratio. Furthermore, these changes are often subject to temperature fluctuations in the laboratory which affects the measurements negatively.

(Knight et al., 1995) developed a method for estimating the critical moisture content that can be implemented on expansive soils. This method relies on measuring the loss of moisture content with time. Drying of porous media has two distinct stages—constant rate and falling rate period. The constant rate period refers to the period of water being evaporated from the macro pores whereas, during the falling rate period, water is leaving the micro pores. During the constant rate period, the rate of evaporation—which is calculated from the rate of moisture loss—is constant and it starts decreasing in the falling rate period.

However, it is also important to note here that critical moisture content is a property investigated and used by mostly agricultural engineers. Therefore, the majority of literature on this parameter is not within the domain of geotechnics. (Kenanoğlu & Toker, 2023) attempted to use critical moisture content to distinguish between 'relatively higher moisture contents' and 'relatively lower moisture contents.' They then proposed that unsaturated tests be carried out at or below critical moisture content to ensure constant water conditions. However, this procedure was validated only for a silty soil.

2.4 Constitutive Modelling of Unsaturated Soils

Throughout the recent decades, various researchers have attempted to develop models for unsaturated soils with varying degrees of success. The most fundamental problem faced by researchers in this domain is the lack of agreement concerning stress state variables i.e. the parameters that can be used to dictate or predict the

strength of soil. There exist two schools of thought in this regard: independent stress state variables and effective stress state variables. In the former category, net stress and suction or degree of saturation are used as the stress state variables whereas, in the latter, suction is accounted for in the effective stress variable and not defined separately.

The independent stress state approach considers two variables that govern the stress-strain behavior of soil i.e. net stress and matric suction. Net stress is the total stress minus air pressure. Matric suction is the air pressure minus water pressure. With this approach, a coupled hydro-mechanical elastoplastic model is needed to evaluate the response of the soil skeleton to applied loads. Also, two sets of material parameters are needed, corresponding to each of the stress state variables.

The most notable model following this approach is the Barcelona Basic Model (BBM) (Alonso et al., 1990). The BBM was formulated as an extension of the Modified Cam Clay (MCC) model. Subsequent models following this approach were all based on the BBM with slight modifications to fit certain soil types (Gens & Alonso, 1992; Alonso et al., 1999; Wheeler & Sivakumar, 1995; Wheeler, 1996; Cui & Delage, 1996; Vaunat et al., 2000; Wheeler et al., 2002; Benatti et al., 2013). In such models, the yield surface is a function of the mean net stress, deviatoric stress, matric suction, apparent isotropic pre-consolidation pressure at the suction value of interest, cohesion intercept and a material constant. As suction increases, the yield surface grows. Therefore, the shear strength of the soil also increases.

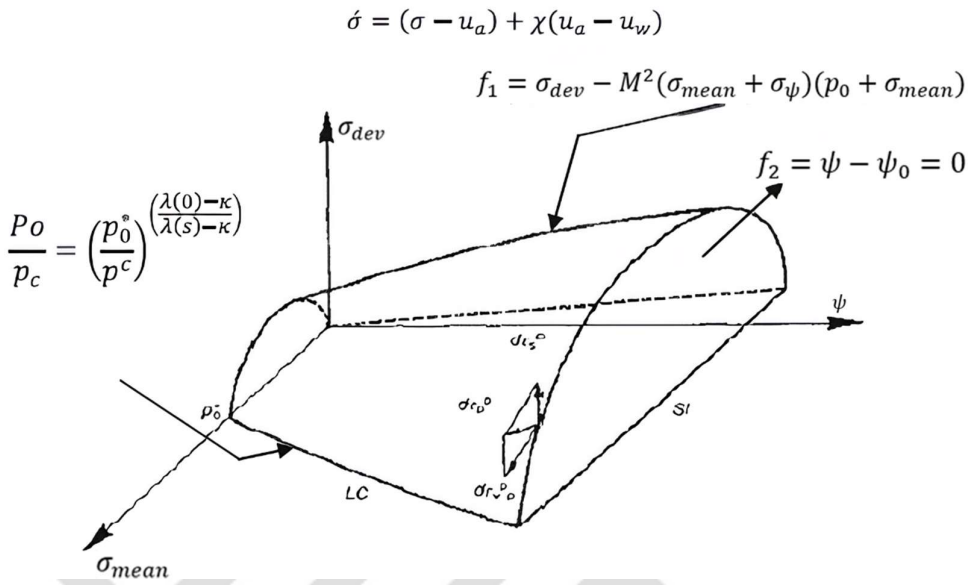

Figure 2.3. Yield surface of BBM

In the above figure, p_c is the reference stress, p_0^* is the pre-consolidation pressure for saturated coniditon, $\lambda(0)$ is the slope of the virgin compression line, $\lambda(s)$ is a function of suction, κ_s is slope of elastic compression line due to suction change, M is the slope of the critical state line.

While the development of this approach was a big step forward in the domain of unsaturated soils, it presents some shortcomings as well. Some of the limitations of this approach include the omission of residual suction and shear strength being linearly dependent on suction (Khallili et al., 2022). It is also important to note that for a true two-state model, strains must be defined for each of the stress state variables separately for all phases of the model such as the elastic model, the yield surface, the flow rule, the hardening model, etc. BBM and its successors do not include any information regarding this (Gallipoli et al., 2010).

On the other hand, the effective stress state approach relies on a single parameter—the effective stress parameter—to govern the stress state behavior. (Bishop, 1959) defined this as:

$$\sigma' = \sigma - p_a + \chi(p_a - p_w) \quad \text{(Eq 2.4)}$$

This parameter already accounts for the effect of suction on the stress, thus eliminating the need for it to be considered separately. Various researchers have attempted to develop equations to define this parameter (see Section 2.5). (Khalili & Khabbaz, 1998) developed the most widely used relationship for the effective stress parameter (χ):

$$\chi = \begin{cases} 1, & \frac{\psi}{\psi_{AEV}} \leq 1 \\ \left(\frac{\psi}{\psi_{AEV}}\right)^{-\lambda}, & 1 \leq \frac{\psi}{\psi_{AEV}} \leq 14 \end{cases}$$

where ψ is the suction, ψ_{AEV} is the air entry value of suction and λ is a fitting parameter equal to 0.55.

Subsequent models based on the effective stress approach have made use of this parameter (Kohgo et al., 1993; Loret & Khalili, 2000; Khalili & Loret, 2001; Khalili et al., 2004; Sheng et al., 2003; Eberhardsteiner et al., 2003; Borja, 2004; Sheng et al., 2004; Ehlers et al., 2004; Russell & Khalili, 2006; Mašín & Khalili, 2008).

With this approach, one can capture the mechanical behavior of the soil solids. In such models, the yield surface is a function of the effective stress and another parameter controlling the size of the yield surface. The MCC model is used to model the plastic strains of soil and a hardening parameter captures the stiffening effect of suction/unsaturation on the soil's solid skeleton.

The world of unsaturated soils is yet to reach a consensus regarding which approach is superior. Typically, researchers tend to select a model based on its input parameters. Different parameters require different types of experimental campaigns. This, combined with the fact that unsaturated experiments require sophisticated equipment that is not commonly available, encourages researchers to pick a model based on the experiments that they can conduct.

Previously, it was believed that independent stress state models required a larger amount of experimental data. Another misconception was that these models could

only be calibrated using constant suction tests. However, (Kenanoğlu, 2023) calibrated BBM using experimental data from constant water tests and was able to produce satisfactory results for silty soil.

2.5 Effective Stress Parameters

As mentioned in the previous section, the effective stress approach makes use of the effective stress parameter to govern the stress state behavior. The most notable and widely used correlation for this parameter—i.e. the one developed by Khalili and Khabbaz (1998)—has been outlined in the previous section. However, throughout the past decades, various other researchers have also attempted to develop correlations for the effective stress parameter. Table 2.2 contains details of some of the equations developed.

Table 2.2 Equations for the apparent cohesions

Reference	Equation
Vanapalli et al. (1996)	$c'' = (u_a - u_w)\frac{S - S_r}{100 - S_r} tan\phi'$
Karube et al. (1996)	$c'' = (u_a - u_w)\frac{\theta - \theta_r}{\theta_s - \theta_r} tan\phi'$
Öberg and Sällfors (1997)	$c'' = (u_a - u_w)\, S\, tan\phi'$
Bao (1998)	$c'' = (u_a - u_w)\frac{\log(\psi)_r - \log(\psi)}{\log(\psi)_r - \log(\psi)_{AEV}} tan\phi'$
Khalili & Khabbaz (1998)	$c'' = (u_a - u_w)\left(\frac{\psi}{\psi_{AEV}}\right)^{-\lambda} tan\phi'$

where c'' is the apparent cohesion, u_a is the air pressure, u_w is the water pressure, S is the degree of saturation, S_r is the residual degree of saturation, θ is the volumetric moisture content, θ_r is the residual volumetric moisture content, θ_s is the saturated volumetric moisture content, ψ is the suction, ψ_r is the residual suction and ψ_{AEV} is the air entry value of suction.

2.6 Previous Studies on Ankara Clay

Ankara clay is a geologically significant soil in Turkey. This is partly due to Ankara being the capital city and a major metropolitan hub of the country and partly due to the unique properties of this soil. Ankara clay is characterized as a fine high-plasticity clay with a reddish brown color. In its in-situ state, it tends to have bits of calcareous concretions or gravel in its layers. Two-thirds of the city of Ankara is built on this soil type, thus giving rise to its importance and developing a need for its properties to be studied extensively (Akbas & Kulhawy, 2010).

It is also expansive in nature, with swelling pressures as high as 131 kPa and free swell percentages up to 115% (Erguler & Ulusay, 2003). This can be especially problematic because, during the rainy season, soil can expand and cause cracks in buildings and other structures. Some studies have been conducted on the swelling nature of Ankara clay and its possible remediation using additives such as lime and silica (Avsar et al., 2009; Tonoz et al., 2004).

Due to its dense and high-plastic nature, Ankara clay also has the potential to be used as a compacted clay liner for landfills (Akgün et al., 2017; Met & Akgün, 2015; Met et al., 2005).

Some studies have also been conducted on the unsaturated properties of Ankara Clay. These studies tend to focus on the shear strength and its relationship with other soil properties such as suction or compaction moisture content (Çokça & Tilgen, 2010; Cokca et al., 2004). Some studies have conducted extensive unsaturated tests on Ankara Clay but those studies tend to focus more on the development of experimental methodologies rather than the properties of Ankara Clay (Kenanoğlu, 2023; Ahmadi Naghadeh, 2016).

However, all current studies on unsaturated Ankara Clay tend to make use of reconstituted specimens. Loose soil is collected from sites and compacted or consolidated in laboratory settings to achieve desired soil properties. While these studies provide us with valuable insights, they cannot accurately capture the behavior

of soil in its in-situ state. This is because, in its in-situ state, Ankara clay experiences extremely high pre-consolidation pressures which cannot be replicated in laboratory settings. Furthermore, while erasing the stress history, the reconstitution of soil can create a new stress history, which is not necessarily realistic (Ahmadi Naghadeh, 2016).

CHAPTER 3

SOIL CHARACTERIZATION

Some basic tests were carried out on both samples in order to determine their properties and to classify them according to the Unified Soil Classification System (USCS). This section describes the samples and the tests carried out on them in detail. Finally, soil classification according to USCS has been done.

The data from the two sites were not merged by any means. The first sample provided an incomplete data set but served as a rough estimate for the second one, whereas the second sample was treated independently with a more extensive testing program.

3.1 Sample Collection

The first sample's location was in the Bahçelievler neighborhood in Çankaya, Ankara. The specimens were taken from an excavation site approximately 3 meters below ground level by pressing shelby tubes into the soil with the bucket of a backhoe excavator.

Another batch of samples was taken from inside the Middle East Technical University (METU) which is located in Çankaya, Ankara. The samples were extracted according to ASTM D1587 with a rotary drill rig by hydraulicly pressing shelby tubes at the bottom of several adjacent boreholes at the construction site of a dormitory building and the depth of extraction ranged from 3 to 5 meters. The largest horizontal distance between any two boreholes was 2 meters.

3.2 Specific Gravity

Specific gravity test was conducted in accordance with ASTM D854 – 02 Method B 'Procedure for Oven Dried Specimens.' For the first sample, three trials were conducted and the final value of the specific gravity was found to be 2.61. The standard deviation was 0.004 which was within the acceptable range. For the second sample, another three trials were conducted and the final value of specific gravity was determined as 2.51.

3.3 Particle Size Distribution

Particle size distribution was determined using a combination of sieve analysis and hydrometer procedures. Upon visual inspection, both samples appeared to consist almost entirely of fine-grained particles. However, a few bits of gravel were spotted, necessitating sieve analysis in addition to the hydrometer.

For each of the two samples, two specimens of known masses were prepared, one for sieve analysis and one for hydrometer. Loose soil was placed in beakers and 20g of sodium hexametaphosphate was added to each beaker along with 200ml of water. The beakers were left overnight in order to allow the sodium hexametaphosphate to dissolve all clumps. At the end of 24 hours, hydrometer test was performed using the sample in one of the beakers in accordance with ASTM D7928 (see Figure 3.1).

Figure 3.1. Hydrometer test

Wet sieving was carried out using the specimen in the other beaker (see Figure 3.2). The soil passing the sieve was allowed to be washed away. The portion of the specimen which was retained on the sieve was then oven-dried. The percentage retained on the sieve was determined using the initial mass of the specimen added to the beaker. Sieve analysis was then carried out with that specimen. The results of the two tests were then combined.

Figure 3.2. Wet sieving

The following particle size distribution was determined for both the samples (see Figure 3.3).

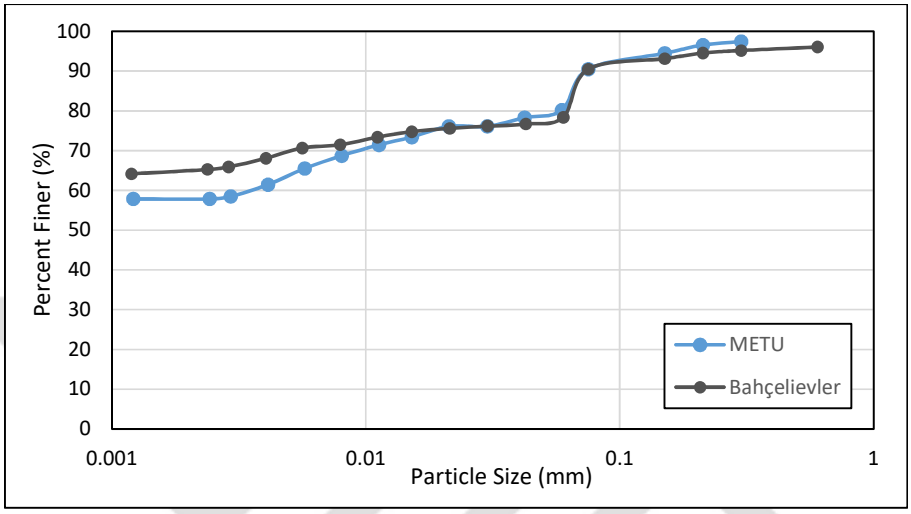

Figure 3.3. Particle size distribution of both samples

As can be seen from the above figure, the majority of both soils are clay-sized particles.

3.4 Liquid Limit, Plastic Limit and Plasticity Index

Liquid and plastic limit of the soil were determined in accordance with ASTM D4318. For liquid limit, the wet to dry approach was used. Furthermore, for liquid limit, Fall Cone Test (FCT) was carried out in addition to the procedure outlined in ASTM standards.

For the first sample, three trials were carried out using Casagrande's apparatus and two using the fall cone (see Figure 3.4). In the former, 3-4 different moisture contents were used whereas in the latter, 5 different moisture contents were used. Graphs of water content versus the number of blows (depth of penetration, in case of fall cone) were plotted in a semi-log scale and the liquid limit was determined. Since the results

of all five trials were within 1% of each other, the average value was taken. The final value of the liquid limit came out as 69.4%.

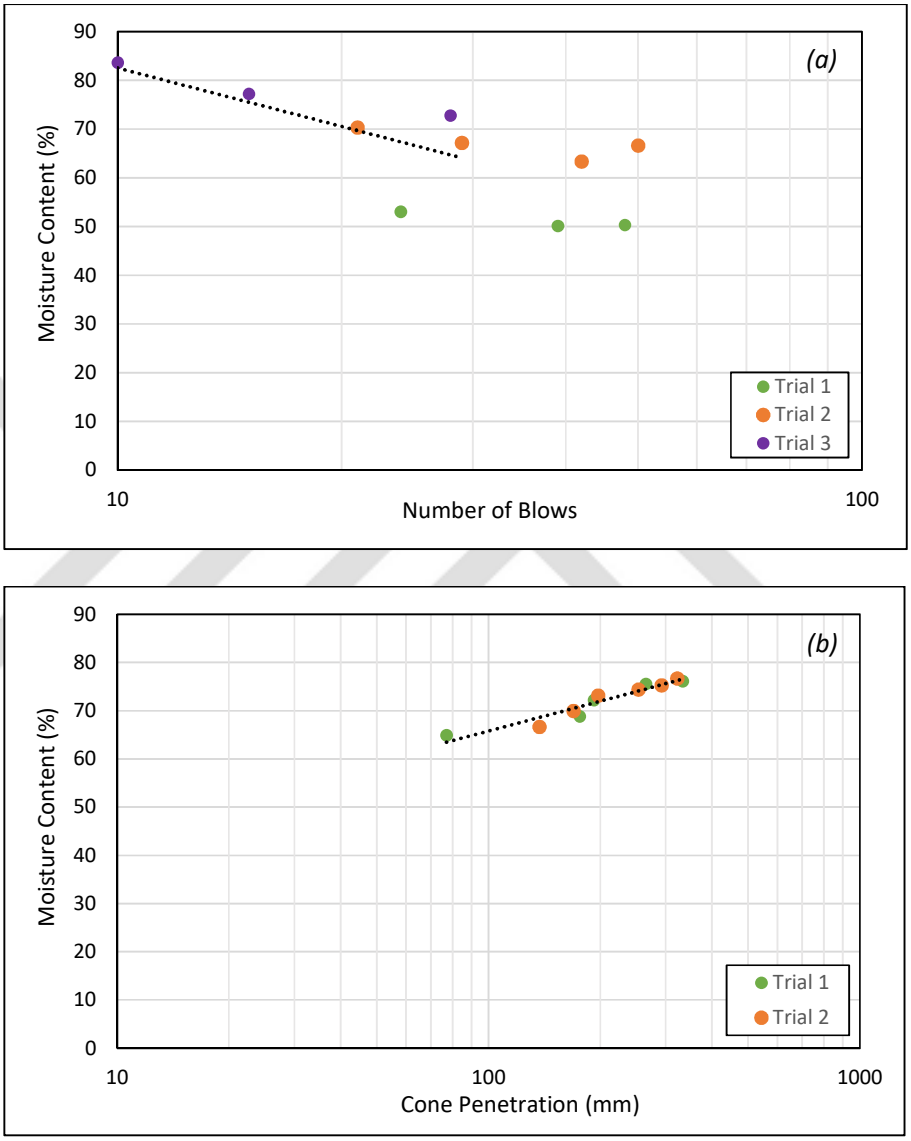

Figure 3.4. Graphs of liquid limit test for (a) Casagrande method and (b) Fall cone method for the Bahçelievler specimen

For plastic limit determination, threads of soil at different moisture contents were rolled out. The threads that broke at exactly 3.2mm diameter were taken for water content determination. A total of eleven such trials were carried out and the average

value was taken. Finally, plastic limit was determined as 39.4%. Consequently, the plasticity index of this specimen was determined as 30.0%.

For the second sample, identical procedures were adopted and Atterberg limits and plasticity index were determined. After the removal of outlier points, liquid limit of this specimen was determined as 81.8%, plastic limit as 27.1% and plasticity index as 54.7%.

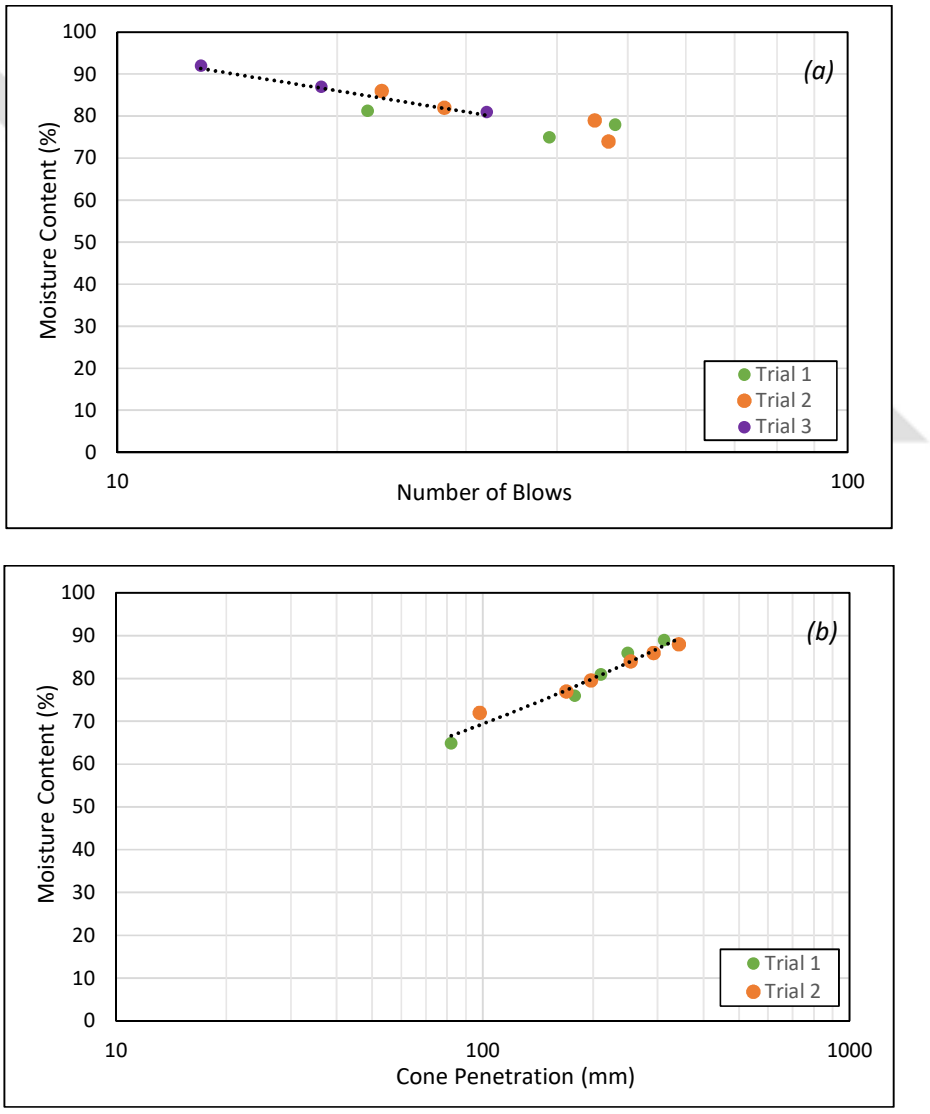

Figure 3.5. Graphs of liquid limit test for (a) Casagrande method and (b) Fall cone method for the METU specimen

3.5 Soil Classification

Based on the results of the index tests, the activity of the soil was also calculated:

$$Activity = \frac{Plasticity\ Index}{\%\ Clay} \quad \text{(Eq 2.1)}$$

A summary of the basic properties of all specimens is presented as follows:

Table 3.1 Summary of Sample Properties

Sample No.	Location	*Gs*	*LL*	*PL*	*PI*	*% Clay*	*% Silt*	*% Sand*	*% Gravel*	*Activity*
1	Bahçelievler	2.61	69.4	39.4	30.0	64.9	25.6	5.1	4.4	0.462
2	METU	2.51	81.8	27.1	54.7	57.9	32.6	7.5	2.0	0.945

The swell potential of the soil was also classified according to the criteria by (Holtz & Gibbs, 1954). The samples were then classified and their soil types were identified according to a few notable soil classification systems.

Table 3.2 Summary of Sample Classification

Sample No.	Location	*USCS*	*AASHTO*	*British Standard*	*Swell Potential*
1	Bahçelievler	High Plasticity Silt	A-7-5	High Plasticity Silt	High
2	METU	High Plasticity Clay	A-7-6	Very High Plasticity Clay	Very High

CHAPTER 4

HYDRAULIC TESTS

Several tests were carried out on the samples of Ankara clay in order to determine its hydraulic properties such as water retention, infiltration, evaporation, etc. These properties are important when analyzing soil from an unsaturated lens. The tests conducted as part of this study were evaporation test, shrinkage curve determination and formulation of SWRC.

4.1 Evaporation Test

Evaporation test was conducted on the second sample of Ankara clay (from METU) in order to determine its critical moisture content. In this study, the method of (Knight et al., 1995) was used because it relies only on the change in mass of the soil as it dries. A specimen of diameter 36mm and height 20mm was cut from a shelby tube sample and saturated in a water bath. The saturated specimen was then covered with a latex membrane on the sides to restrict moisture loss in the lateral direction. Therefore, evaporation was only allowed from the top surface of the specimen.

The membrane-covered specimen was then placed on top of a mass balance with a precision of 0.001g in order to track changes in mass (see Figure 4.1). A webcam was placed in front of the mass balance which took screenshots of the mass reading every 30 minutes. A table lamp was also placed to prevent the screenshots from getting too dark at night time. Once the mass of the specimen became constant, the test was stopped and the specimen was oven-dried in order to retroactively obtain gravimetric water content from all mass readings.

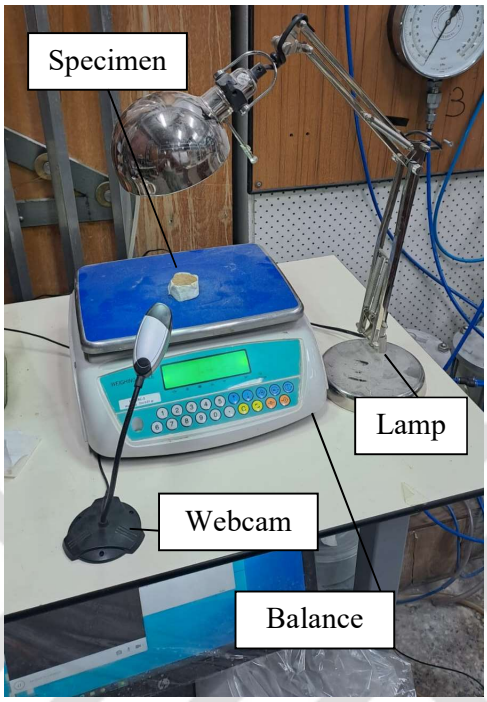

Figure 4.1. Evaporation test setup

Moisture content versus time graph was then plotted (see Figures 4.2 and 4.4). The graph displayed a linear trend in the beginning but flattened out eventually. The period of the linear trend is known as the constant rate period as the rate of drying is constant. After the constant rate period, is the falling rate period where the drying rate monotonically decreases. A linear trend line was fitted to the constant rate period. Moisture content values were then calculated from the trend line and the relative deviation between them and actual moisture content values was calculated. The formula for relative deviation is as follows:

$$Relative\ Deviation = \frac{w_i(t) - w(t)}{w(t)} \quad \text{(Eq 3.1)}$$

where $w_i(t)$ is the moisture content calculated from the linear trendline and $w(t)$ is the actual moisture content.

The data points which have a relative deviation of less than 0.01 were deemed to be in the constant rate period. The data points that have a relative deviation of greater

than 0.01 were in the falling rate period. Finally, the transition between the two regimes i.e. the data point which had a relative deviation of exactly 0.01 was designated as the critical moisture content. In summary,

Relative deviation < 0.01 = constant rate period
Relative deviation = 0.01 = critical moisture content
Relative deviation > 0.01 = falling rate period

Firstly, a trial was conducted but it delivered unsatisfactory results (see Figure 4.2). This was due to the fact that the starting moisture content was too low.

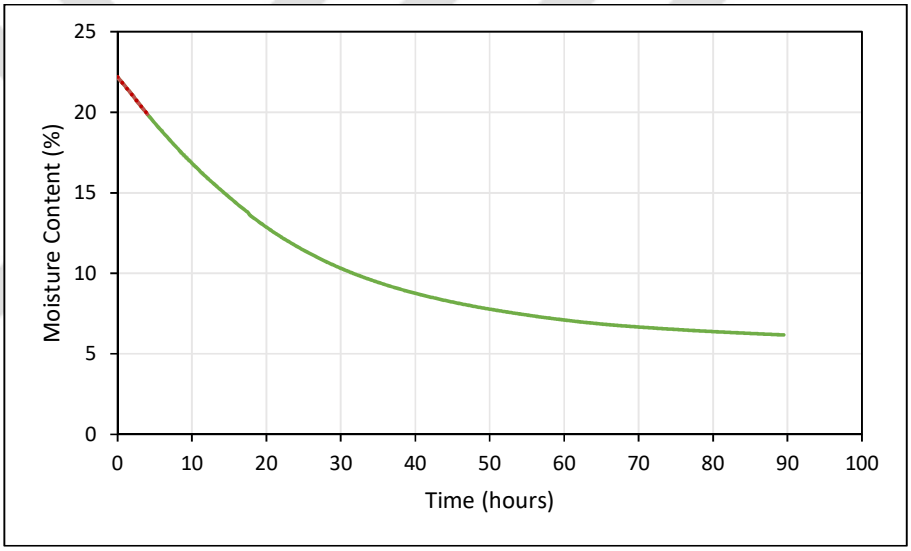

Figure 4.2. Moisture content versus time plot of the unsuccessful evaporation test on the METU sample

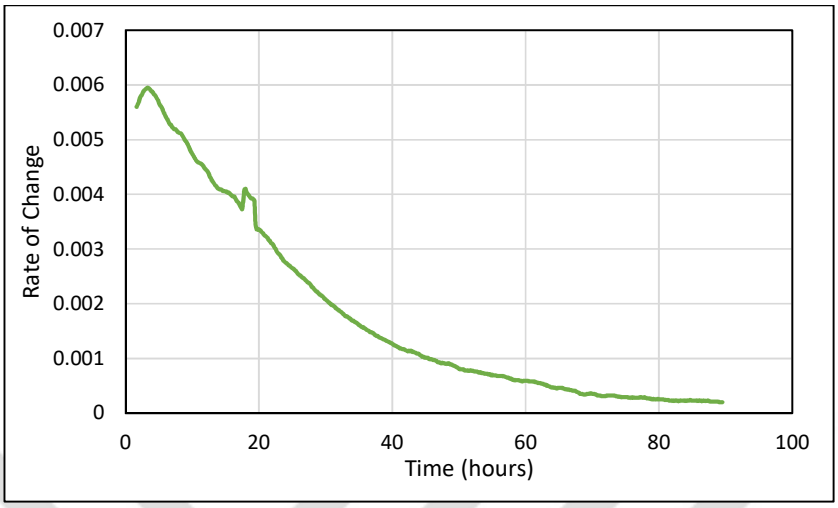

Figure 4.3. Moisture content versus time plot of the unsuccessful evaporation test on the METU sample

Subsequently, another trial was conducted with a higher initial moisture content moisture content (see Figures 4.4 and 4.5). This was ensured by wrapping the specimen in filter paper and placing it in a mold. The mold was then placed in a water bath to saturate the specimen. Care was also taken to ensure that the specimen was not left out of the water bath too long prior to starting the test. In this trial, value of relative deviation started from -0.02 and increased further along.

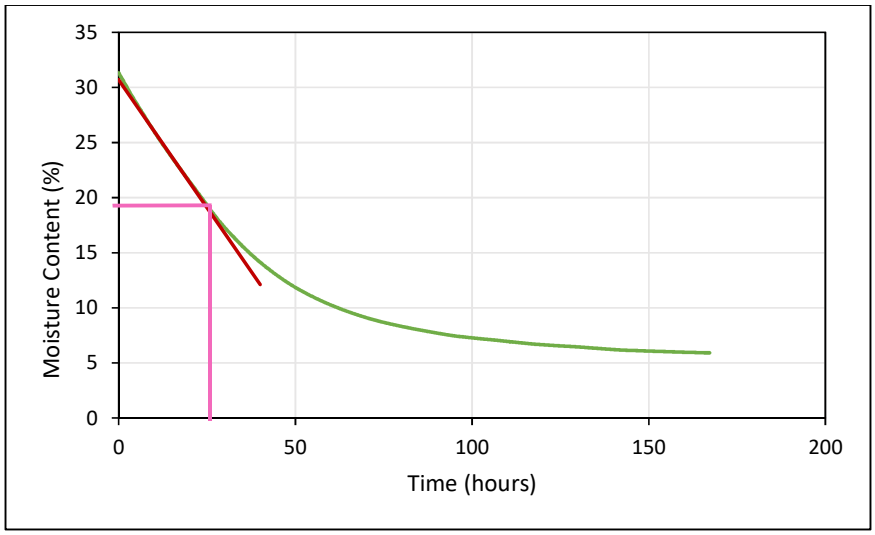

Figure 4.4. Results of the successful evaporation test on the METU sample

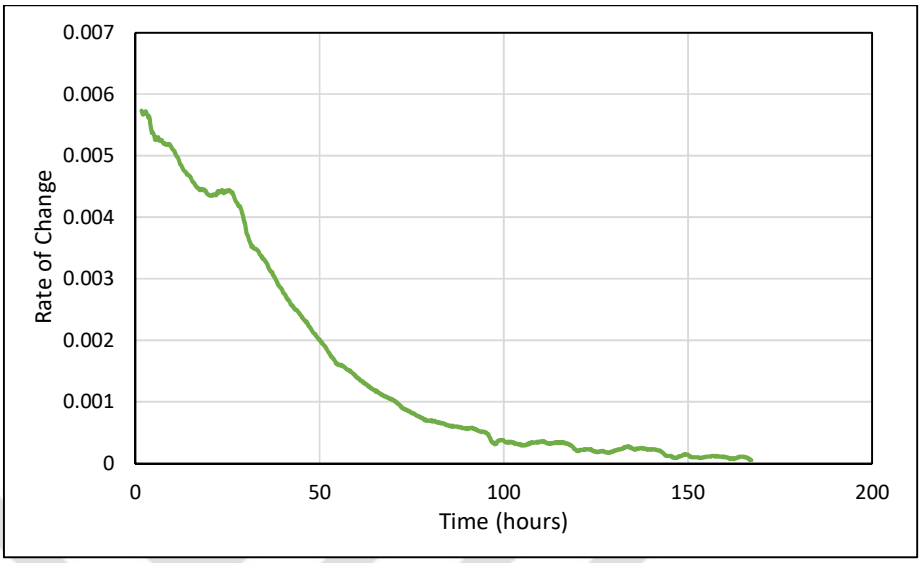

Figure 4.5. Moisture content versus time plot of the successful evaporation test on the METU sample

From this trial, critical mositure content of the METU sample of Ankara clay was determined as 19.75%.

4.2 Shrinkage Curve

Ankara clay is an exapnsive soil which indicates that its void ratio changes significantly with change in moisture content. Therefore, it is imperative to know the void ratio at different moisture contents to enable accurate determination of properties such as volumentric water content and degree of saturation. For this purpose, shrinkage curve of the second sample of Ankara clay was determined which depicts the trend of void ratio with change in gravimetric water content.

Saturated specimens were air-dried for various durations in order to obtain a variety of moisture contents. Drying was carried out for 2 hours per day after which specimens were completely covered in plastic wrap and placed in a humidity room. This was done to avoid shrinkage cracks in the specimen which can alter the volume measurement. Covering with plastic wrap allowed the specimens to come to

equilibrium after drying which helped to close any micro cracks that had developed during the drying process.

Once specimens had dried to the desired degree, their volume was determined using the water displacement method. The procedure is as follows:

- Cut specimen into half and keep one half for water content measurement
- Measure the mass of the other half of the specimen (M_1)
- Coat the second half of the specimen in paraffin wax and wait for it to cool down
- Measure mass of the wax covered piece (M_2) (see Figure 4.6 (c))
- Measure the mass of beaker with water only (M_3)
- Assemble a beaker with a suspension system (see Figure 4.6 (d)) and measure the mass of the empty system without specimen as reference (M_4)
- Submerge the wax covered piece in the water such that the suspension system is not touching the beaker at any point, without entrapping any air bubbles
- Measure the mass of beaker with the submerged specimen (M_5)
- Measure the temperature of water to determine ρ_w
- Calculate the volume as follows:

  $M_2 - M_1$ = mass of wax

  $V_{wax} = \frac{M_{wax}}{\rho_{wax}}$ where ρ_{wax} is taken as 2.88

  $\frac{M_4 - M_3}{\rho_w} = V_{tray}$

  $M_5 - M_3$ = uplift force on the tray + wax coated specimen

  $\frac{M_5 - M_3}{\rho_w} = V_{total}$

  $V_{soil} = V_{total} - V_{tray} - V_{wax}$

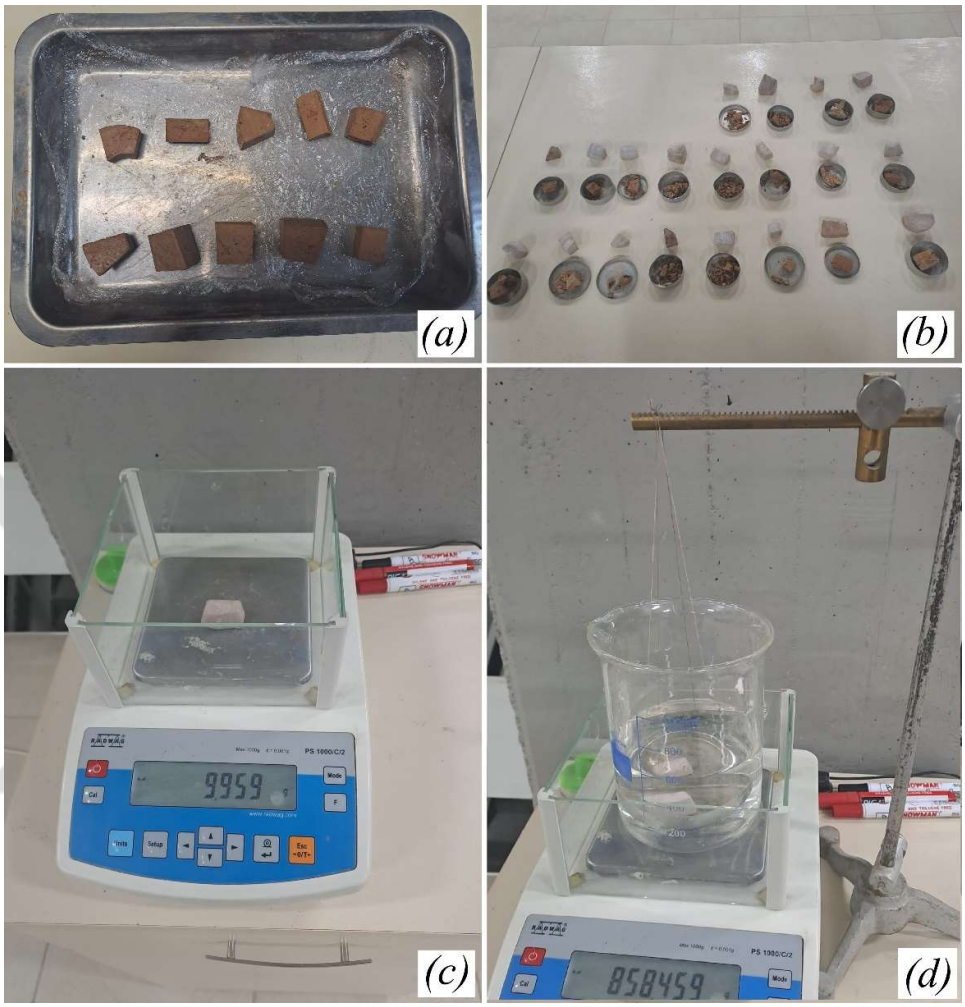

Figure 4.6. Air dried specimens (a), wax covered specimens and water content tares (b), measurement of mass of wax covered specimen (c) and measurement of submerged mass of wax covered specimen (d)

Once all the measurements are taken, bulk density of soil is determined which is then used to compute void ratio. Void ratio versus moisture content graph is plotted (see Figure 4.7). The equation of (M. Fredlund et al., 2002)is fitted to the data:

$$e(w) = a\left(\left(\frac{w}{b}\right)^{c} + 1\right)^{1/c} \quad \text{(Eq 3.2)}$$

where w is the gravimetric water content and a, b and c are constants which were determined as 0.322, 0.130 and 30.268 respectively for the second sample.

Afterwards, some specimens were wetted to various degrees and the same procedure was repeated in order to obtain the wetting branch of the shrinkage curve and capture the hysteris. The shrinkage limit of was also obtained from this curve which corresponded to a moisture content of 12.5%.

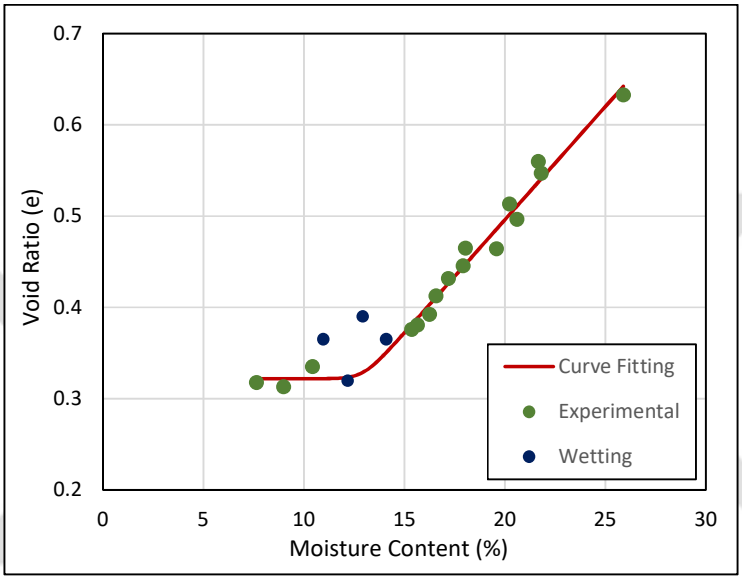

Figure 4.7. Shrinkage Curve for the METU specimen

4.3 Soil Water Retention Curve

Soil water retention curve was determined for the second sample of Ankara clay at this specific void ratio of 0.658. Two methods were utilized for this purpose, namely axis translation and vapor euilibirum techniques. Axis translation was used for low suctions (upto 900 kPa) and vapor quilibrium was used for high suctions (upto 90,000 kPa).

4.3.1 Axis Translation

Axis translation was carried out in a suction controlled oedometric cell. The cell is equipped with a 15 bar high-air entry (HAE) ceramic at the bottom of an air-tight chamber. Beneath the ceramic, there is a spiral groove base to allow passage of water

through drainage lines which are then connected to a beaker filled with water. Air pressure is applied from the top of the cell in order to achieve the desired level of suction (see Figure 4.8). Specimen is placed inside the cell and air pressure is applied while the water lines connected to the beaker are at 0 kPa gage pressure. Hence, the value of air pressure applied is equal to the value of the suction.

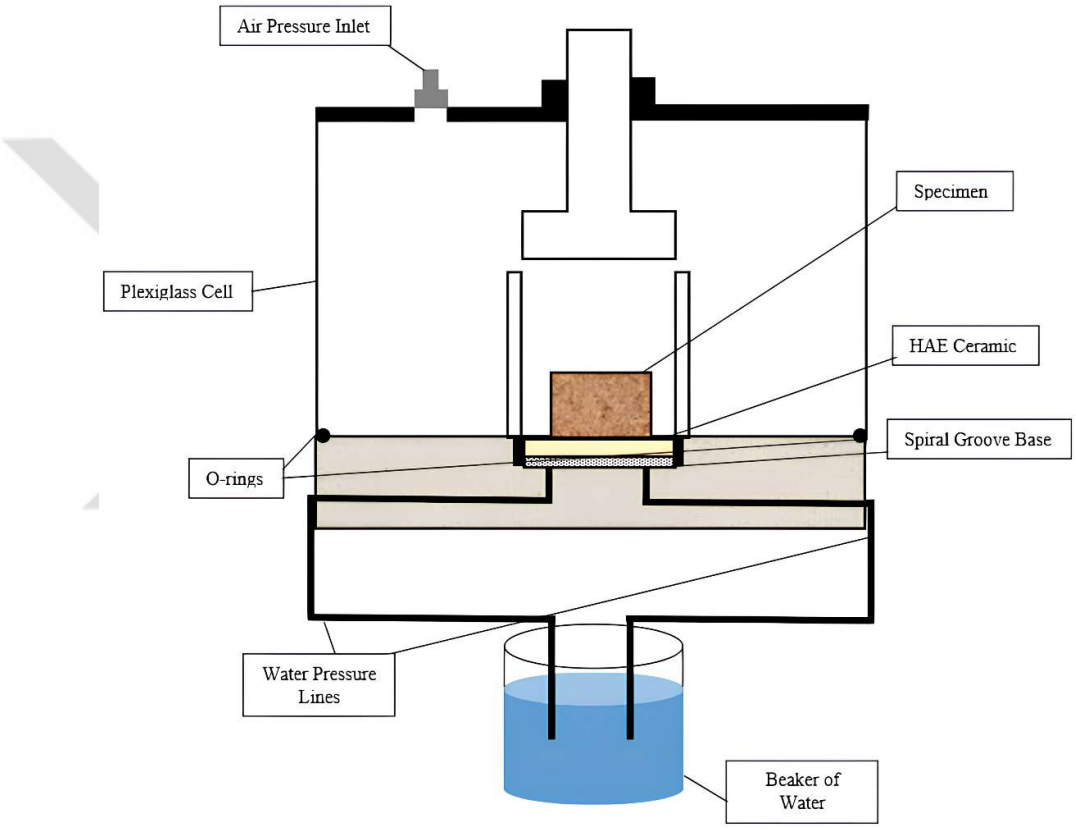

Figure 4.8. Schematic diagram of axis translation setup

Figure 4.9. Axis translation setup

A specimen with 36mm diameter and 20mm height was cut from the undisturbed shelby tube samples. The specimen was then saturated in the water bath and placed in the cell. Various increasing levels of suction were applied—i.e. 60, 100, 200, 400 and 800 kPa—and equilibrium was achieved at each suction. Equilibriation durations were taken from Kenanoğlu (2023) and, for points on the drying curve, this duration was 7 days. After the specimen reached equilibrium, it was specimen was taken out of the cell and its weight, height and diameter were measured.

Once the drying curve was complete, the specimen was first air-dried for a week and then oven-dried for a day. This was done to prevent shrinkage cracks from appearing on the specimen. The dried specimen was then placed inside the cell again and suction was applied. For the wetting curve, suction levels were applied in a decreasing trend i.e. 700, 400, 200 and 100 kPa. According to Kenanoğlu (2023), equilibrium duration for each point on the wetting curve was 20 days. Once it had

been achieved, specimen was taken out and its weight, height and diameter was once again measured.

While the specimen was equilibiriating at each value of suction, the water inlet pipes were flushed with water everyday using a syringe. This is because air dissolved in the water can diffuse through the HAE ceramic disc. This causes air bubbles to accumulate at the bottom of the disc, preventing the specimen from drawing or releasing water into the disc. At high levels of suction, this process was carried out twice a day.

4.3.2 Vapor Equilibrium

For high suction application, vapor equilibrium technique was used. This technique utilizes saturated salt solutions in air-tight jar. The salt solution imposes a certain level of relative humidity in the jar, depending on the temperature. This, in turn, imposes a calculable total suction on the soil specimen placed in the jar. The values of relative humidity with temperature were found from tables in (Greenspan, 1977) and the corresponding suctions were calculated from the Kelvin equation:

$$\psi = \frac{-\gamma_w RT}{(MW)_w} \ln(RH) \qquad \text{(Eq 3.3)}$$

where ψ is the suction in kPa, γ_w is the density of water, (MW)w is the molar weight of water (18.016 g/mol), R is the ideal gas constant, T is the temperature in Kelvin scale and RH is the relative humidity in decimal form.

Five salt solutions were used for both wetting and drying curves. An initial trial was carried out with just one temperature control chamber. Specimens were wetted by spraying them with water and wrapping them in plastic wrap for one week . For the drying curve, specimens were air-dried for a week. The specimens were placed in jars which were then put in a refrigerator for temperature control. However, the results of this trial contained discrepancies, particularly in the wetting curve. Hence, this trial was discarded and another trial of vapor equilibirum was carried out with

additional temperature conrol chambers and a more effective method for wetting of the specimens (see Section 3.3.2.1).

In the second trial, three different methods for temperature control were used, namely a refrigerator (4.1 °C), a low-temperature oven (40 °C) and an air-tight cooler box (14.1 °C) placed at room temperature were used. Details of salt solutions and their imposed suctions can be found in Table 4.1. Once again, five salt solutions were employed for suction imposition separately for both wetting and drying curves at each of the three temperatures. Hence, a total of (5x3x2=) 30 specimens were used.

Table 4.1 Salt solutions and their corresponding suctions at different temperatures

T	Salt									
	K2SO4		KNO3		KCl		NaCl		NaBr	
°C	RH (%)	Suction (kPa)	RH (%)	Suction (kPa)	RH (%)	Suction (kPa)	RH (%)	Suction (kPa)	RH (%)	Suction (kPa)
4.5	98.51	1920	96.30	4820	87.76	16697	75.65	35689	63.65	57781
14.1	97.94	2751	95.51	6079	86.07	19842	75.62	36970	60.94	65517
40	96.41	5273	89.03	16759	82.32	28061	74.68	42109	53.17	91107

For the wetting curve, specimens were air dried for a month. For the drying curve, specimens were wetted as described in 3.3.2.1. Once wetting and drying had been completed, specimens were placed inside the jars such that they were not in contact with the salt solution. This was achieved by using makeshift stands (see Figure 4.10). The jars were then sealed with nylon, as well as their lid, and placed in their respective temperature control chambers. Saturation of salt solutions was ensured by having excess of the salts in the jars, such that precipitation is visible. In each of the temperature chambers, a sealed container of water was also placed. At the end of the experiment, the temperature of the water was measured and all salt solutions in the same temperature chambers were assumed to be at the same temperature.

Figure 4.10. Vapor equilbirum specimens on stands inside jars

Two control jars were also placed at room temperature, one for wetting and one for drying curve. For the wetting and drying curve control jars, the salt solutions were NaBr (which imposed a suction of 65517 kPa) and K_2SO_4 (which imposed a suction of 2751 kPa), respectively. Each week, the mass of the specimens was measured and when mass stopped changing equilibrium was assumed to be achieved. For the wetting curve, specimens achieved equilbirium in a week. For the drying curve, specimens took 7 weeks to achieve equilbrium.

Once equilbirum was achieved in all of the specimens, they were removed from their jars and moisture content was determined. In this way, the 'tail-end' of the retention curve was determined for Ankara clay.

4.3.2.1 Wetting of specimens

For the drying curve, fully saturated specimens are required. However, the specimens for vapor equilibrium were irregularly shaped and therefore could not fit into any of the moulds that could be placed in the water bath. Hence, a new technique for wetting of irregularly shaped specimens was developed.

Specimens were covered from all sides in strips of filter paper that had been saturated beforehand (see Figure 4.11 (a)). Then the specimens were wrapped in plastic wrap and left in the humidity room. In this way, specimens in the range of 15g to 25g were fully wetted in 24 hours. This was verified by cutting several specimens to ensure that they had been wetted to their cores. Upon cutting, surface water was visually observed on the specimens, thus confirming full sauration and complete elimination of suction (see Figure 4.11 (b)).

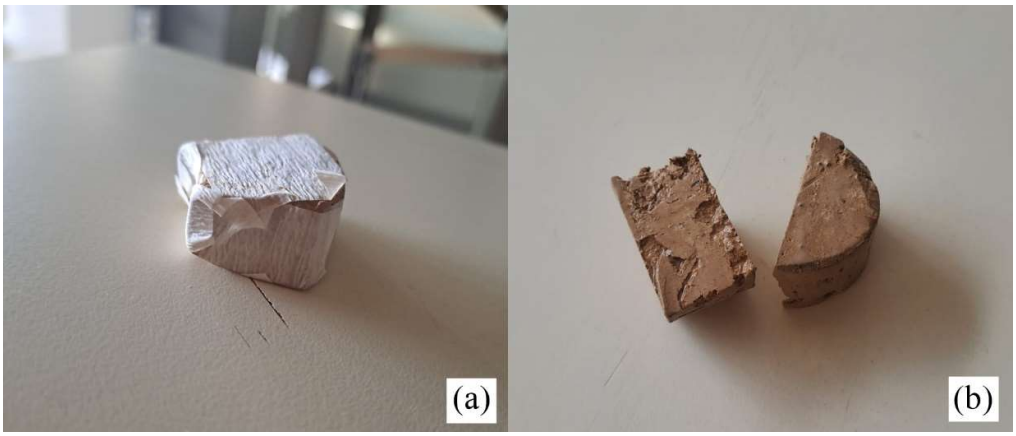

Figure 4.11. (a) filter paper covered specimen for wetting and (b) wet specimen unwrapped from filter paper

4.3.3 SWRC of Ankara Clay

The results of the axis translation and vapor equilbirium techniques was combined in order to obtain a complete retention curve of Ankara clay. Mass measurements for gravimetric water content were taken at the end of the axis translation and vapor equilbirium experiments. For volumteric water content and degree of saturation, the shrinkage curve developed in section 2.2 was used. Using the value of gravimetric water content, the void ratio was inferred from the curve and volumetric water content and degree of saturation were calculated from basic formulas. The retention curve was developed for gravimetric water content, volumetric water content and degree of saturation (see Figures 4.12 (a), (b) and (c)).

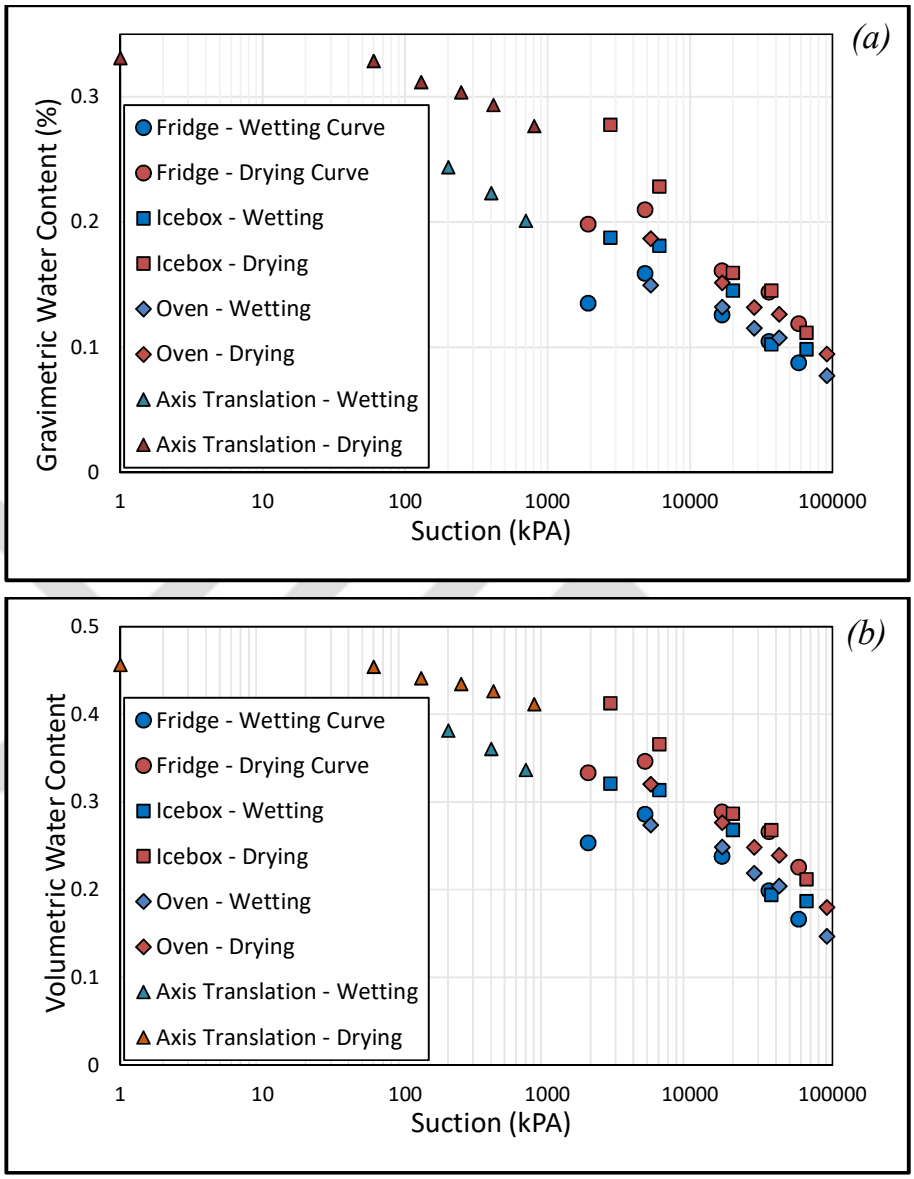
(a)
Gravimetric Water Content (%)
0
0.1
0.2
0.3
1
10
100
1000
10000
100000
Suction (kPA)
Fridge - Wetting Curve
Fridge - Drying Curve
Icebox - Wetting
Icebox - Drying
Oven - Wetting
Oven - Drying
Axis Translation - Wetting
Axis Translation - Drying
(b)
Volumetric Water Content
0
0.1
0.2
0.3
0.4
0.5
1
10
100
1000
10000
100000
Suction (kPA)
Fridge - Wetting Curve
Fridge - Drying Curve
Icebox - Wetting
Icebox - Drying
Oven - Wetting
Oven - Drying
Axis Translation - Wetting
Axis Translation - Drying

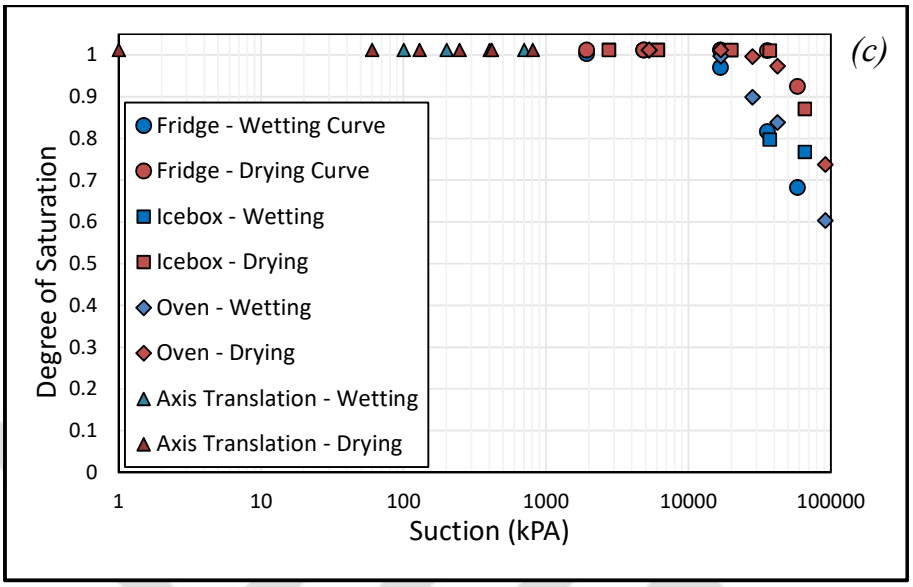

Figure 4.12. Soil water retention curve of the METU sample in terms of (a) gravimetric water content, (b) volumetric water content and (c) degree of saturation

As can be seen from the above figures, the air-entry value of suction is 38000 kPa on the drying curve. This corresponds to a gravimetric water content of 13% and a volumetric water content of 25%.

It is also noteworthy that the air-entry gravimetric moisture content of 13% is close to the shrinkage limit of 12.5%, thus lending credibility to the results of the two experiments.

Additionally, the SWRC was also plotted against void ratio, as shown in Figure 4.13:

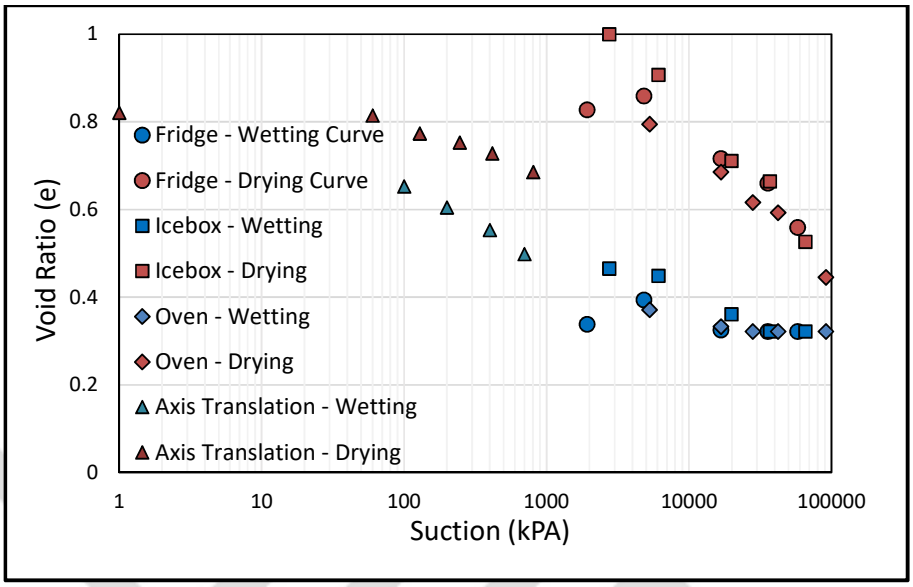

Figure 4.13. Soil water retention curve of the METU sample against void ratio

CHAPTER 5

MECHANICAL TESTS

Strength tests were carried out on the specimens in order to evaluate their strength properties in both saturated and unsaturated states. These tests include triaxial and oedometric compression tests.

5.1 Saturated Tests

A series of saturated tests were conducted on the specimens in order to discern their saturated properties such as shear strength and pre-consolidation pressure. The results of these tests were meant to be used in conjunction with the results of the unsaturated tests in order to get a better picture of the strength properties of soil.

5.1.1 Consolidation Test

Consolidation tests were carried out on both samples of Ankara clay in accordance to ASTM D2435-04. Specimens measuring 63mm in diamter and 20mm in height were soaked in an oedometer cell. The saturated specimens were then loaded in increments and settlement behaviour of soil was recorded. Each loading stage was continued for 24 hours and, using settlement data, void ratios at the end of primary consolidation for each loading stage were calculated. Void ratio versus stress graph was plotted on a semi-log scale.

For the Bahçelievler specimen, the loading schedule was 1-10-25-50-100-200-400-800-1600-400-100-400-1600-2000 kPa. These results of this test can be seen in Figure 5.1. From this graph, properties of the soils were calculated such as pre-consolidation pressure using the Casagrande method (140 kPa), compression index (0.171) and swelling index (0.061).

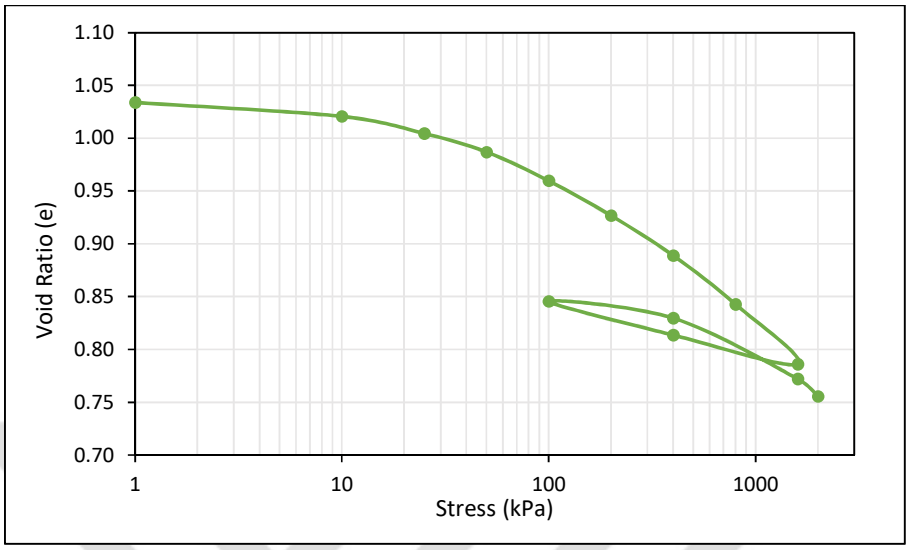

Figure 5.1. Compression curve for the Bachelievler sample

For the METU specimen, the loading schedule used was 1-69-139-277-554-693-554-277-554-693-1247 kPa. The results of this test can be seen in Figure 5.2. From this graph, soil properties were calculated as: pre-consolidation pressure (200 kPa), compression index (0.092) and swelling index (0.018).

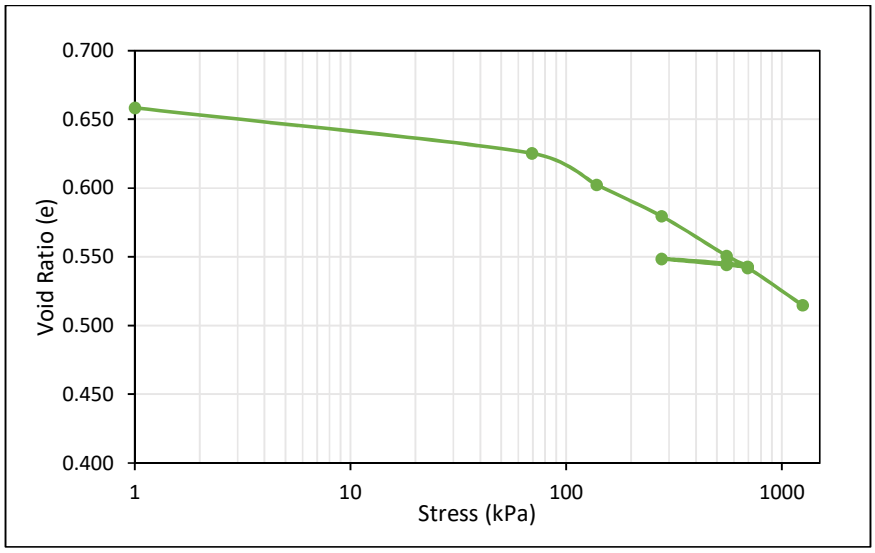

Figure 5.2. Compression curve for the METU sample

5.1.2 CD Triaxial Tests

CD triaxial tests were first attempted on the Bahçelievler specimen. However, the samples proved to be too brittle and, hence, reasonably sized triaxial specimens could not be extruded from the shelby tubes. First, extrusion of specimens with diameter 50mm and height 100mm was attempted. Then, smaller specimens of 36mm diamter and 72mm height were also attempted but to no avail. Therefore, triaxial tests were only carried out on samples from METU. This was also the main reason for acquiring for the METU sample.

5.1.2.1 Development of Water Bath for Saturating Specimens

The specimens, in their in-situ state, experienced high amounts of suction and proved difficult to saturate in the triaxial setup. Filter strips as side drains and pressures as high as 1000 kPa were used but B-value of 0.95 was not achieved. Thus, a water bath was developed for this purpose (see Figure 5.3).

The water bath consists of specimens in perforated mold and covered on top and bottom by porous stones. Filter paper was placed between the specimen and the perofrated mold in order to prevent the soil from expanding through the holes of the mold. A load (of approximately 2 kgs) was placed on top of the top porous stone in order to prevent vertical expansion. This setup was submerged in water until the top of the perforated mold. The top porous stone was not submerged in water to allow the air in the specimen to escape to the atmosphere.

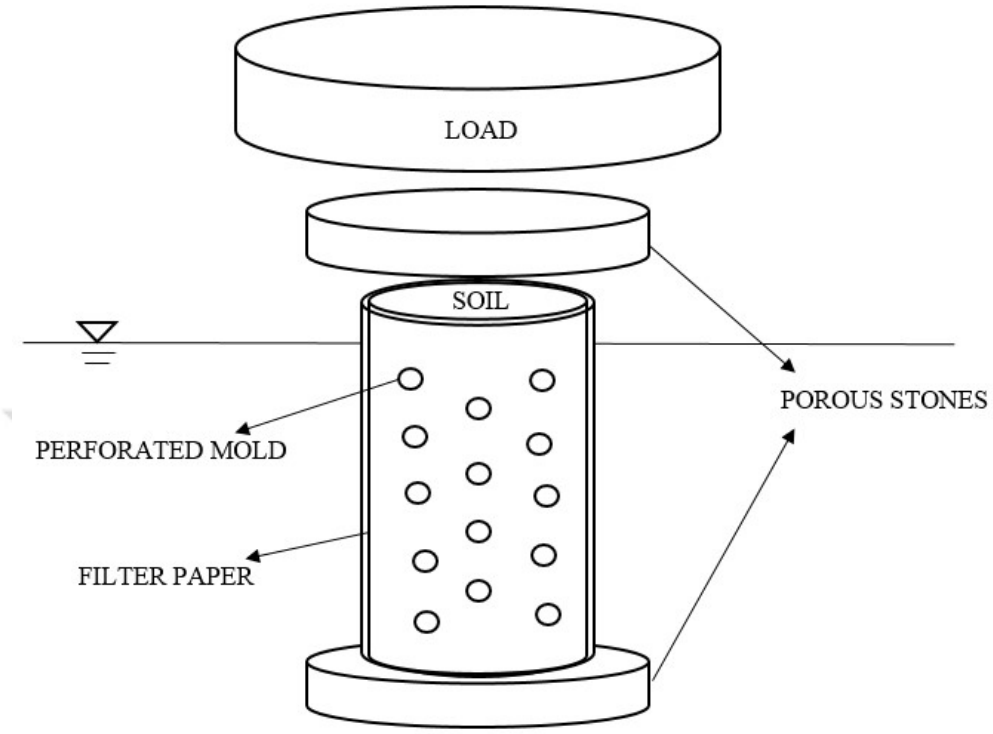

Figure 5.3. Water bath for saturating specimens

In this way, specimens were saturated without accruing any change in volume. Approximate time for saturation was 20 hours. Once specimens were removed from the mold, they were immidiately put in the triaxial chamber in order to prevent expansion in all directions. Specimens that were saturated in this manner before starting the triaxial test reached B-values of 0.95 at pressures as low as 50 kPa.

5.1.2.2 Test Procedure

Conventional saturated CD triaxial tests were conducted at 100 and 400 kPa confining pressures. As mentioned in the previous section, specimens were saturated in a water bath prior to the start of the test and B-value of 0.95 was reached. Consolidation was then carried out, at 100 kPa for the first specimen and 400 kPa for the second specimen. Table 5.1. lists the values of moisture content and void ratio at the beginning of the tests as well as the end of each stage within the tests.

Table 5.1 Moisture content and void ratio values at the beginning and after each stage of the CD triaxial tests

Test Stage	Moisture Content (%)		Void Ratio	
	100 kPa	400 kPa	100 kPa	400 kPa
Beginning	35.9	28.84	0.878	0.756
Initialization	36.7	29.98	0.879	0.756
Saturation	36.9	51.11	0.880	0.762
Consolidation	34.9	32.75	0.413	0.340
Shearing	32.8	30.94	0.401	0.387

After consolidation was complete, shearing was carried out. The strain rate for shearing was determined using the method of (Bishop & Henkel, 1964) and based on the assumption that failure would occur at 8% strain:

$$C_v = \frac{\pi h^2}{100 t_{100}} \quad \text{(Eq 3.4)}$$

And

$$t_f = \frac{20 h^2}{\eta C_v} \quad \text{(Eq 3.5)}$$

Where C_v is the coefficient of consolidation, t_{100} is the time taken for primary consolidation, h is half of specimen height and η was taken as 35.

In this way, the shear rate was calulated as 0.003848%/min and 0.001616%/min for the 100 and 400 kPa tests, respectively. For the 100 kPa test, the consolidation was completed in 1.3 hours and the shearing took 3 days. In the 400 kPa test, the consolidation stage was completed in 5.5 hours and the shearing stage in 5 days.

5.1.2.3 Test Results

At the end of the test, visible failure planes were seen in both of the tests at failure, as shown in Figure 5.4.

Figure 5.4. Failure plane in CD triaxial test on METU specimen

Stress strain graphs were then plotted for both of the tests (see Figure 5.5) as well as Mohr's circles and strength envelope (see Figure 5.6). As can be seen, the peak shear strength of the was 79.86 kPa and 635.93 kPa for the 100 and 400 kPa test respectively.

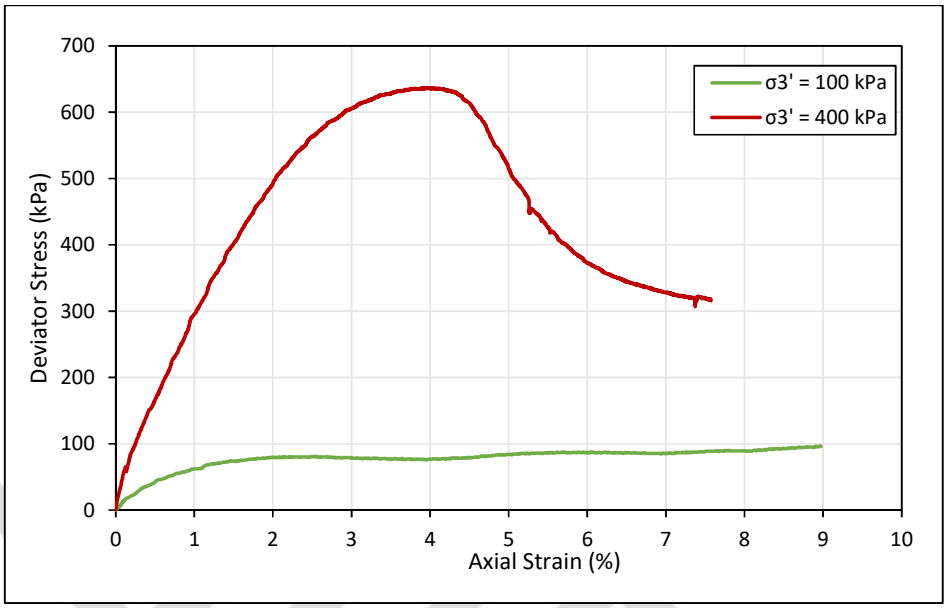

Figure 5.5. Deviator stress versus axial strain graphs for 100 and 400 kPa total confining stress CD triaxial on the METU sample

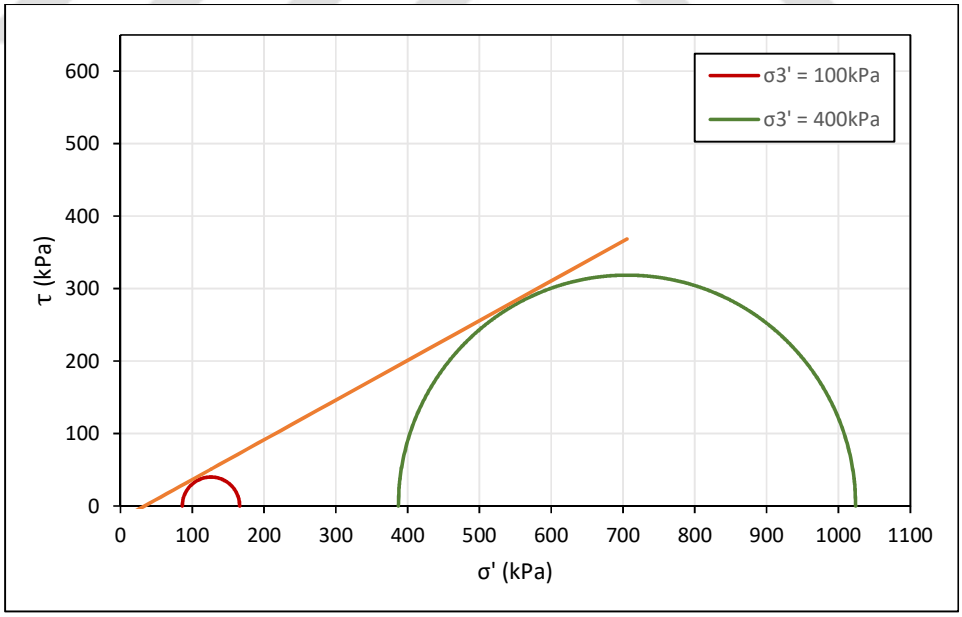

Figure 5.6. Mohr's circles and strength envelope from CD triaxial tests on METU sample

From the above graph, the value of c' was calculated as -18.25 kPa and ϕ' as 28.72°. The negative value of cohesion can likely be attributed to the fact that the 100 kPa sample was overconsolidated whereas the 400 kPa one was normally consolidated.

The slope of the critical state line (M) was also determined from the mean stress-deviator stress space as 1.14 (see Figure 5.7).

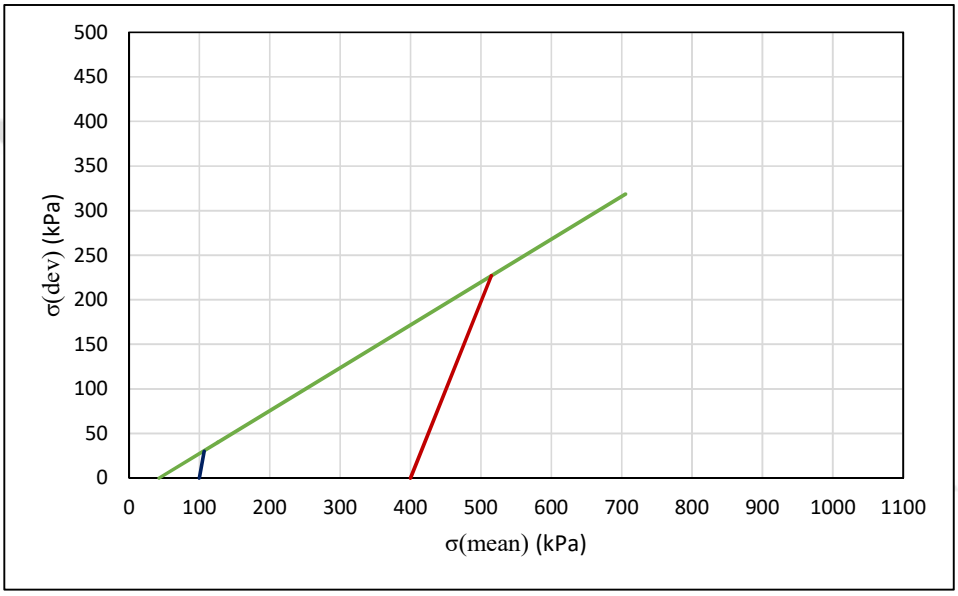

Figure 5.7. Volumetric compressive strain versus axial strain plot during shearing stages of triaxial tests on METU sample

Volumetric compressive strain versus axial strain graphs were also plotted, as shown in Figure 5.8.

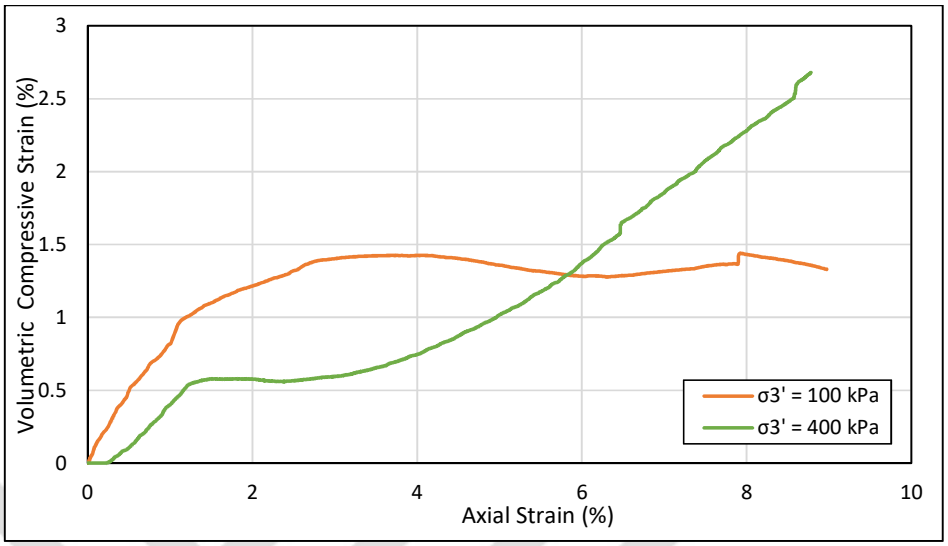

Figure 5.8. Volumetric compressive strain versus axial strain plot during shearing stages of triaxial tests on METU sample

5.2 Unsaturated Tests

Unsaturated oedomteric and triaxial tests were planned to be carried out on the METU sample. However, this sample proved to have extremely high amounts of suction, even in its unsaturated state. Therefore, constant water content tests were carried out rather than constant suction tests.

However, the constant water content tests needed to be carried out on a variety of moisture contents in order to fully capture the behaviour of this sample at various stages of unsaturation. This meant that the specimens had to be dried to varying degrees before they could be tested. The drying of expansive clays can prove be a problematic procedure because it introduces shrinkage cracks in the specimens and also causes them to shrink in size. This is problematic because the shrinkage cracks can act as pre-determined failure planes during shearing. Additionally, the specimens shrink to a smaller size which leads to them disconnecting from the retaining rings in oedometers.

Two different methods were tried out for cutting of triaxial and oedometer specimens. For triaxial tests, specimens were cut using molds that were slightly larger than the required size. The specimen size required for the triaxial was 36mm so specimens were cut by a 38mm cutting tube and then dried. For oedometer tests, samples were extruded from the shelby tubes in bulk, dried to the required degree and then cut to the required size using a cutter with a 30° edge angle and 2.5 mm thickness.

The specimens were then dried to the moisture contents at which unsaturated tests were to be conducted. Since the in-situ moisture content of the sample was 28-30%, the highest value picked was 29%. The lowest moisture content value was selected as 9%, since 10% was the shrinkage limit as determined by the shrinkage curve test. An intermediate value of 19% was also selected.

Additionally, during the drying process, all specimens were dried for approximately two hours each day. This is because, during trials, it was seen that, after two hours, shrinkage cracks started to appear on the surface so they were wrapped in plastic wrap and placed in a humid room to equilibriate. In the final procedure, once the specimens were dried to the required degree, they were again left to equilibriate, this time for a month, to ensure even distribution of moisture content throughout the specimens.

5.2.1 Oedometric Compression Test

Unsaturated oedometric tests were carried out on three specimens at varying moisture contents—i.e. 10%, 18% and 28%. These moisture contents were actually meant to be identical to the values selected in Section 5.2.1. However, moisture contents calculated at the end of the tests revealed these values. The proedcure followed was the same as standard oedometers minus the soaking of the specimen. Furthermore, the oedmoeter cells were convered with plastic wrap in order to prevent

moisture loss (see Figure 5.9). Drainage of water out of the specimen was further restricted by using dry filter paper and porous stones.

Figure 5.9. Oedometer test setup for unsaturated specimens

The loading schedule followed was 69-138-277-554-1108-2216-3325-1108-277-69 kPa. In unsaturated oedometric compression tests (both constant suction and constant water content tests), the common practice is for the loading to exceed the amount of suction present in the specimen (Wheeler & Sivakumar, 1995). However, for this soil, it was not possible—particularly at lower moisture contents—as putting large amounts of weights manually on the machine was logistically impossible. Therefore, a loading schedule was adopted such that it reflected the loads likely to be experienced by the soil in the field.

Compressions curves were then plotted for all three specimens.

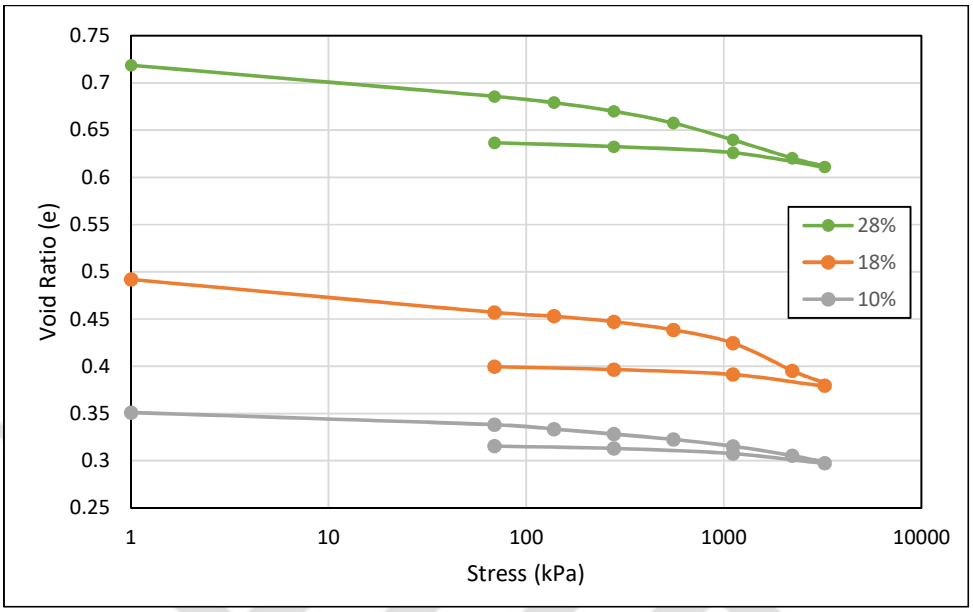

Figure 5.10. Compression curves for the unsaturated oedometric compression tests on the METU sample

Compression index and swelling index was calculated for each of the compressions curves as shown in Table 5.2. Values of the indices from the saturated tests were also added for comparison.

Table 5.2 Compression index and swelling index for saturated and unsaturated oedometric compression tests

Moisture Content	*Cc*	*Cs*
Soaked (25%)	0.0920	0.0180
28%	0.0620	0.0087
18%	0.0968	0.0068
10%	0.0388	0.0066

5.2.2 UU Triaxial Test

Unsaturated Unconsolidated-Undrained (UU) Triaxial tests were planned to be carried out at three different moisture contents—i.e. 9%, 19% and 29%--and two different confining pressures—i.e. 100 kPa and 400 kPa. However, the specimens, in their unsaturated states had high amounts of suction along with some shrinkage cracks—due to being dried—and, therefore, kept breaking during handling and assembly of the test.

Therefore, only five tests were carried out successfully before samples ran out. For 9% and 19% moisture content, two tests each were carried out at 100 kPa and 400 kPa confining pressures. However, for the 29% moisture content, only one test was carried out at 100 kPa confining pressure.

UU tests were carried out by omitting the saturation and consolidation phases. An initial pressure equal to the confining pressure was applied and then specimen was sheared at a strain rate of 1% per minute, which was selected in accordance with ASTM D2850-15. Air drainage was permitted throughout the test by opening the drainage valve to the atmosphere (see Figure 5.11). Inside the test setup, movement of water out of the specimen was restricted using dry filter paper and dry porous stones at the top and bottom. Furthermore, filter strips were not used in order to make it more difficult for the water to drain out of the specimen.

Figure 5.11. Unsaturated UU triaxial setup with air drainage valve open

Stress strain graphs as well as mohr's circles were then plotted for all tests conducted (Figure 5.12 to 5.15) .

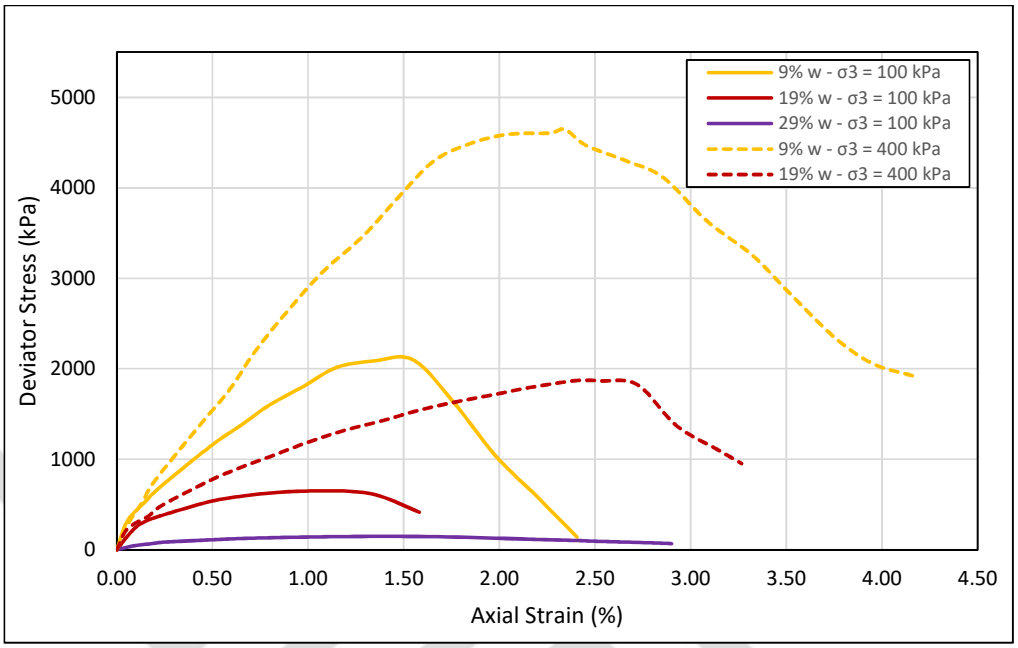

Figure 5.12. Deviator stress versus axial strain plots for UU triaxial tests for the METU sample

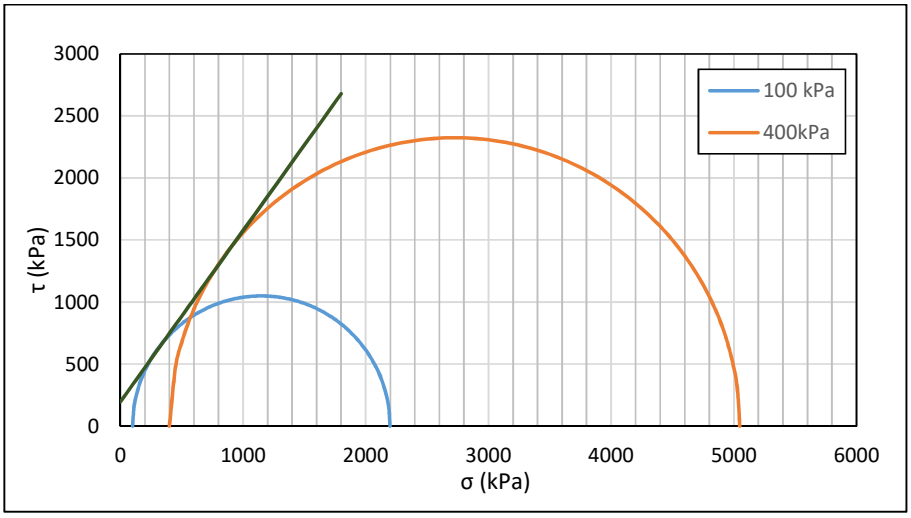

Figure 5.13. Mohr's circles and strength envelope for the 9% water content UU triaxial tests at σ_3 = 100 kPa and 400 kPa on the METU sample

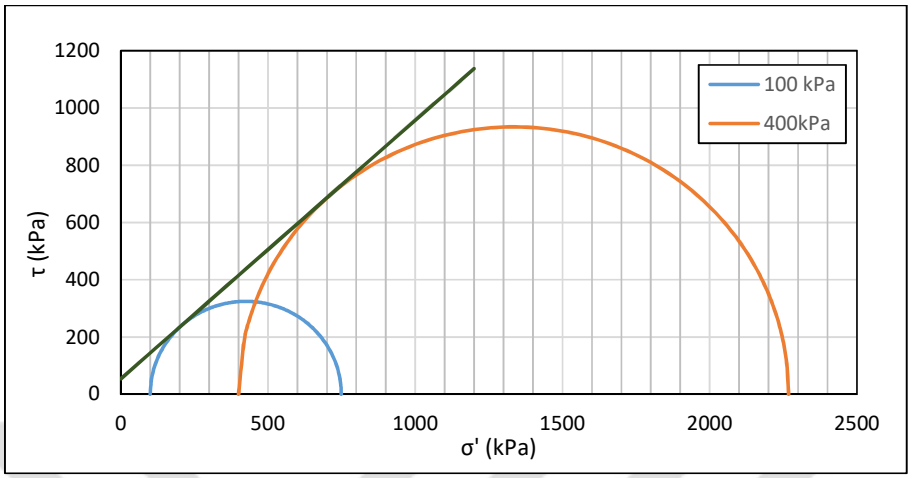

Figure 5.14. Mohr's circles and strength envelope for the 19% water content UU triaxial tests at σ_3 = 100 kPa and 400 kPa on the METU sample

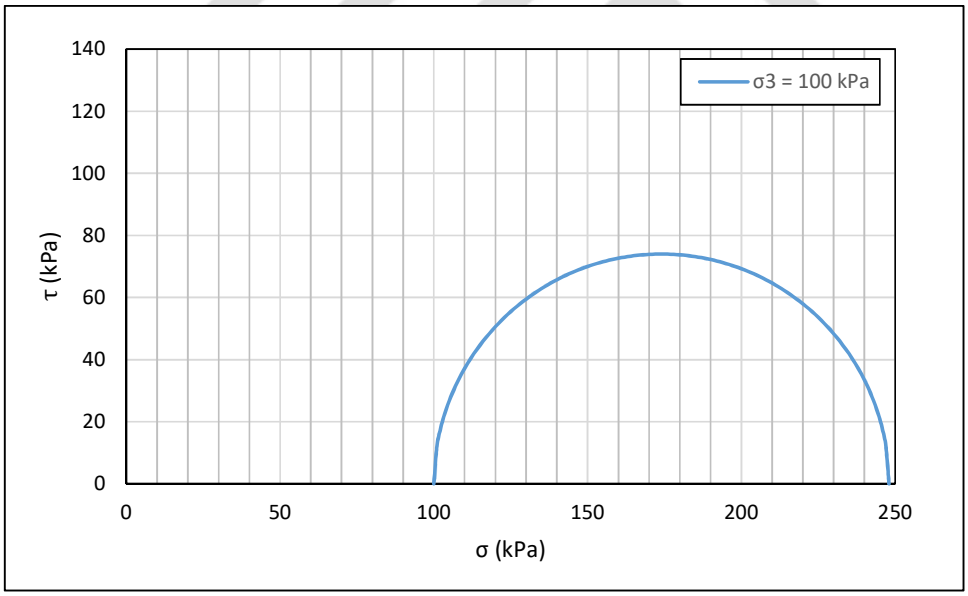

Figure 5.15. Mohr's circle for the 29% water content UU triaxial test at σ_3 = 100 kPa on the METU sample

Finally, the strength envelopes for the unsaturated tests were combined with those of the saturated CD triaxial test and plotted on the same plot to visualize the changes in friction angle and total cohesion with change in suction (see Figure 5.16). Table 5.3

details the values of friction angle and total cohesion for each of the three failure enevelopes.

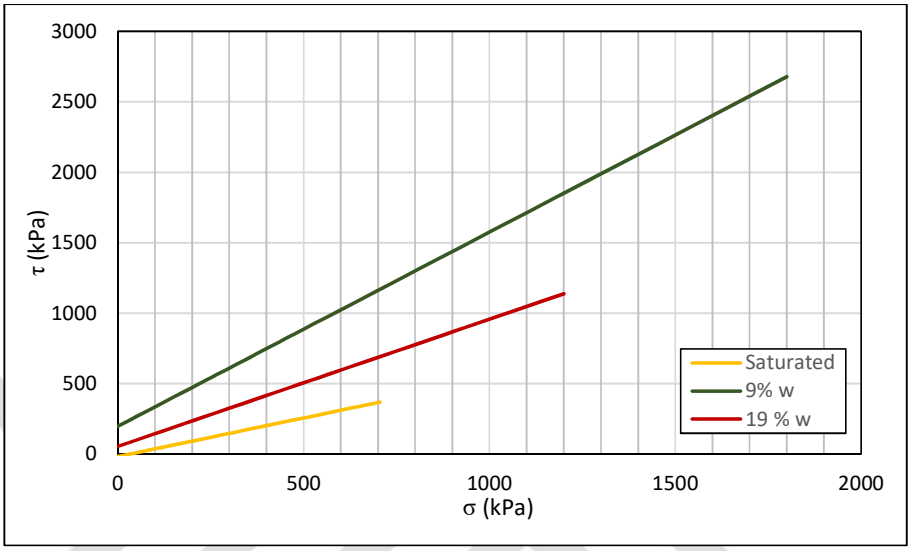

Figure 5.16. Strength envelopes for various moisture contents for the METU sample

Table 5.3 Values of total cohesion and friction angle for each strength envelope in Fig 5.14

Moisture Content	c	ϕ
Saturated (30.9 – 32.8%)	-18.25	28.72
19 %	53.89	42.08
9 %	196.39	54.05

The values of friction angle obtained from the above results appear to be greater than what is normally expected for clayey soils. However, some research indicates that, for high-plasticity clays, values of friction angle in the range of 20-30 degrees are commonly observed (Aubeny, 2002); (Dìaz-Rodrìguez, 1992).

Furthermore, an increase in friction angle can be seen with an increase in suction. This can be due to the fact that, since the specimen is being sheared very fast, suction

is not being developed on the shear plane. When shear plane develops during the test, suction in that shear plane is considerably less than the rest of the specimen, owing to the relatively larger gaps between particles. Furthermore, due to the fast shearing rate, water held in the pores is not being allowed to move towards the shear plane. The decrease in pore water over the shear plane likely also contributes to an increase in friction angle.

This increase in friction angle can also likely be partly attributed to the decrease in void ratio with an increase in suction. Decreasing void ratio indicates a more densely packed soil, thereby leading to better particle interlocking. Furthermore, increasing suction contributes to increasing apparent cohesion which brings soil particles together. This likely leads to better interlocking of soil particles which contributes to an increase in friction angle.

It may also be argued here that confining stress has the same effect but this is not normally reflected in the form of high values of friction angle in other studies. The justification for this would be that, in the current study, the value of suction is changing in order of magnitude which is likely why the friction angle increases as well. Normally, in other studies, confining stress is changed by a few hundred kPa only which is not a big enough increase to contribute to a significant increase in friction angle.

CHAPTER 6

INTERPRETATION OF RESULTS

6.1 Soil Water Retention Curve

The equation be developed by (Van Genuchten, 1980) was fit to the SWRC data:

$$\theta = \theta_{res} + \frac{\theta_{sat} - \theta_{res}}{(1+(\frac{\psi}{\psi_{aev}})^{n})^{m}} \quad \text{(Eq 6.1)}$$

where, θ is the volumetric water content, θ_{sat} is the saturated volumetric water content, θ_{res} is the residual volumetric water content, ψ is the suction, ψ_{aev} is the air-entry value of the suction and n and m are fitting parameters.

38000 kPa was used for ψ_{aev} and the value of θ_{sat} was kept as 45.6%. Ideally, the value of θ_{res} would also be obtained from the experimental data. However, for this soil sample, it was not possible. Therefore, θ_{res} was also kept as a fitting parameter along with m and n.

Optimization was carried out using the drying curve data and the following values of fitting parameters were obtained:

Table 6.1 Values of fitting parameters for the SWRC

Parameter	Value
θ_{res}	0.047
n	0.55
m	1.05

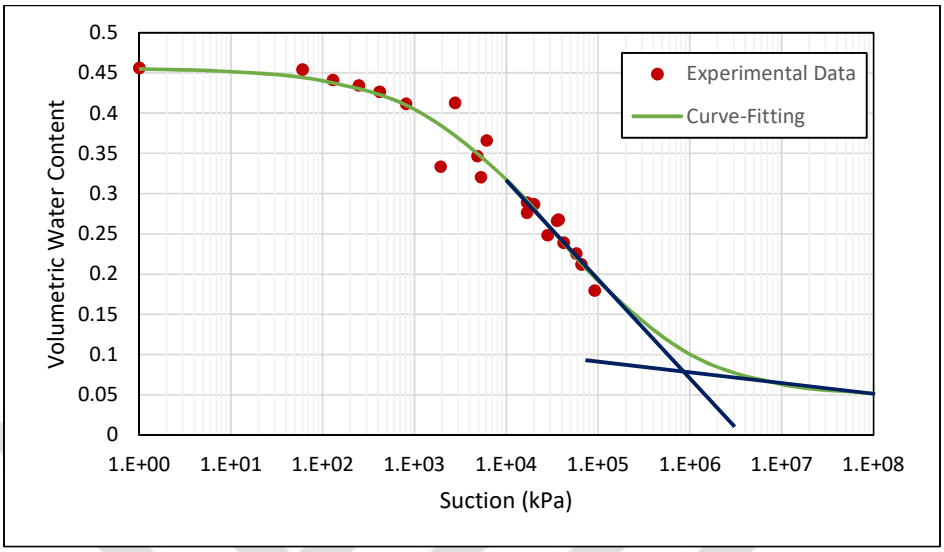

Figure 6.1. SWRC developed after curve-fitting

From the developed curve, the residual values of the volumetric water content and suction were determined as 0.103 and 900000 kPa, respecitvely.

6.2 Strength Envelope

The results of the UU triaxial tests were plotted in a σ-τ-ψ space (see Figure 6.2). Values of ψ corresponding to each moisture content were obtained from equation 6.1. Table 6.2 details the values of suction for each moisture content.

Table 6.2 Values of suction corresponding to moisture contents of constant water content UU triaxial tests

Moisture Content (%)	Ψ (kPa)
29	520
19	7100
9	80000

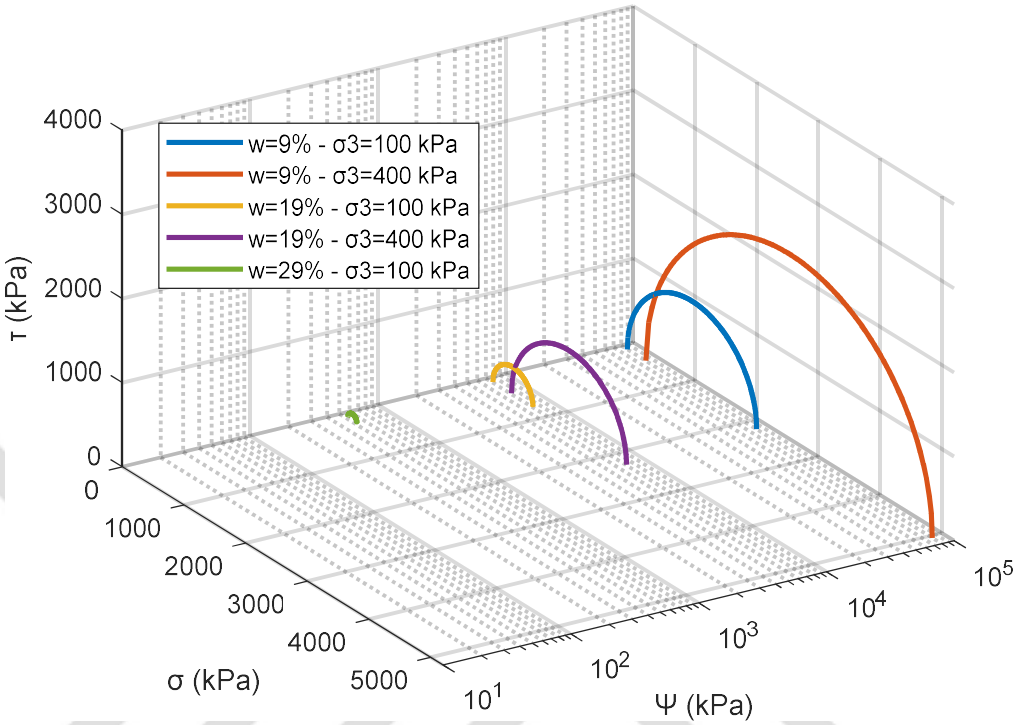

Figure 6.2. Results of the UU triaxial tests in a σ-τ-ψ space

Afterwards, the results of the CD triaxial tests were also incorporated in the above plot (see Figure 6.3). This was done by converting the effective stress in the CD triaxial tests into total stress for a suction value of 10 kPa, which is low enough that total saturation and, therefore, the validity of the effective stress principle is assured. This had to be done for the sake of plotting this diagram on a logarithmic stress scale.

Consequently, for the saturated CD triaxial tests, assumed value of suction acts as negative pore water pressure. Hence, it was added to the values of p' to obtain the values of p:

$$\sigma = \sigma' + u = \sigma' - \psi \qquad \text{(Eq. 6.2)}$$

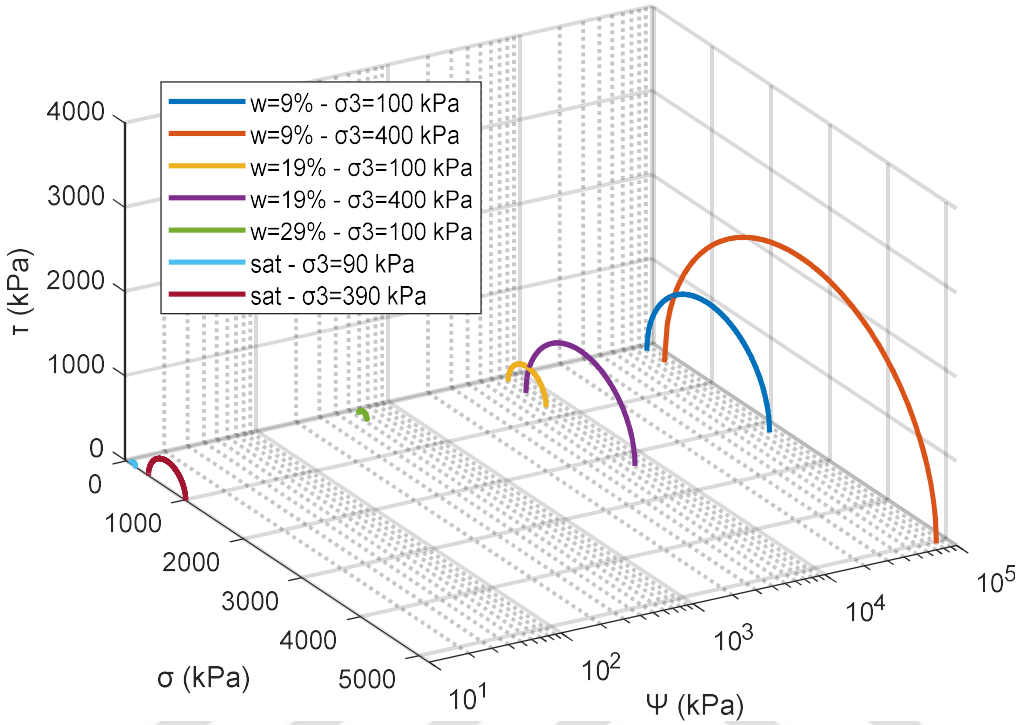

Figure 6.3. Results of the UU triaxial and modified CD triaxial tests in a σ-τ-ψ space

The strength envelopes of all the mohr's circles were then connected and a surface plot was plotted, as shown in Figure 6.4. The top points of the Mohr's circles were also fit to the equation of a plane:

$$q = a_0 + a_1 p + a_2 \psi \qquad \text{(Eq 6.3)}$$

where p is the mean stress and q is the deviator stress.

Seven sets of values of q, p, and ψ were obtained from the peaks of the mohr's circles and the above equation was fit to that data using optimization and values of a_0, a_1 and a_2 were obtained:

Table 6.3 Values of fitting parameters for Eq 6.3

Parameter	Value
a_0	-87.9 kPa
a_1	0.75353
a_2	0.00397

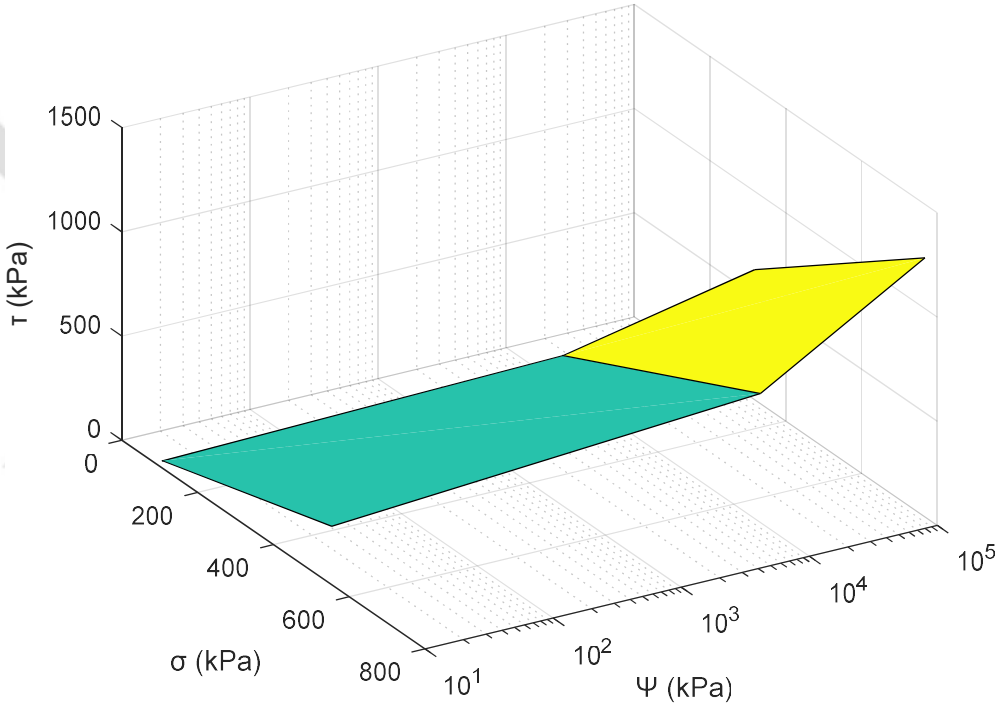

Figure 6.4. Surface plot connecting the strength envelopes of the mohr's circles in a σ-τ-ψ space

The surface plot in Fig 6.4 was then superimposed on the mohr's circles in Fig 6.3 (see Figure 6.5).

Using Eq 6.3, the constants in the equation of shear strength developed by (Fredlund & Morgenstern, 1977) were found:

$$\tau = c' + \sigma' tan\phi' + \psi tan\phi_b \qquad \text{(Eq 6.4)}$$

where τ is the shear strength, σ is the effective stress, c' is the effective cohesion, ψ is the suction, ϕ' is the friction angle and ϕ_b is the shear strength contribution due to matric suction.

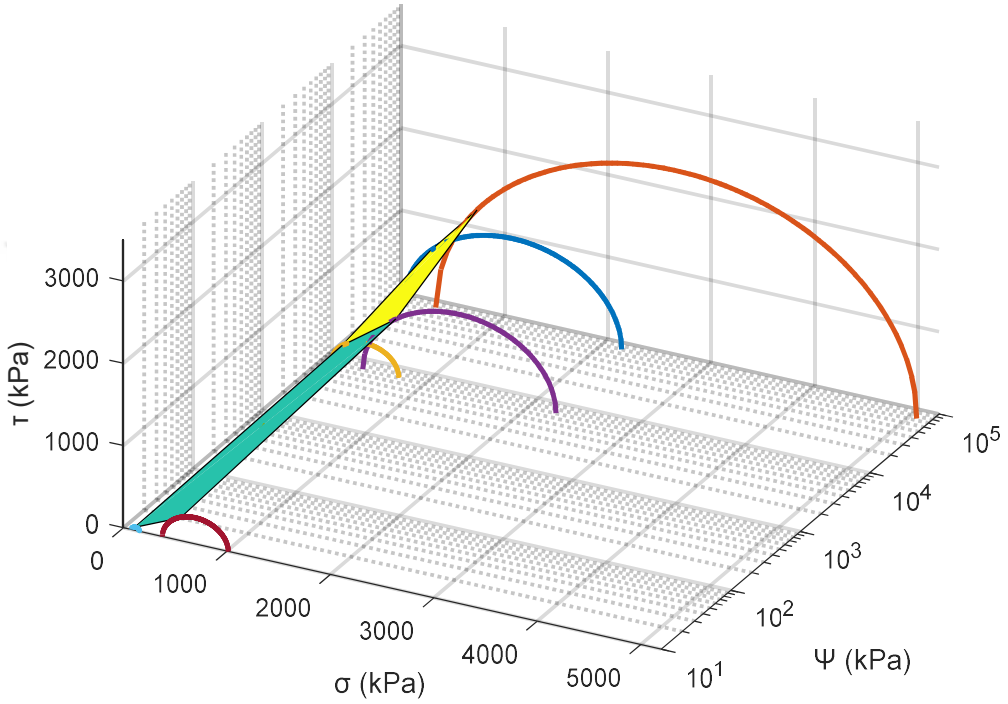

Figure 6.5. Surface plot connecting the strength envelopes of the mohr's circles in a σ-τ-ψ space

Values of c', ϕ' and ϕ_b can be obtained from Eq 6.3 as follows:

$$a_0 = \frac{c'}{cos\phi'}$$

$$a_1 = sin\phi'$$

$$a_2 = tan\phi_b$$

Table 6.4 Values of constants in Eq 6.4

Parameter	Value
c’	-57.8 kPa
ϕ ‘	48.9
ϕ_b	0.227

The surface plot connecting the strength enevelopes of the Mohr’s circles was plotted one again using the results of this optimization.

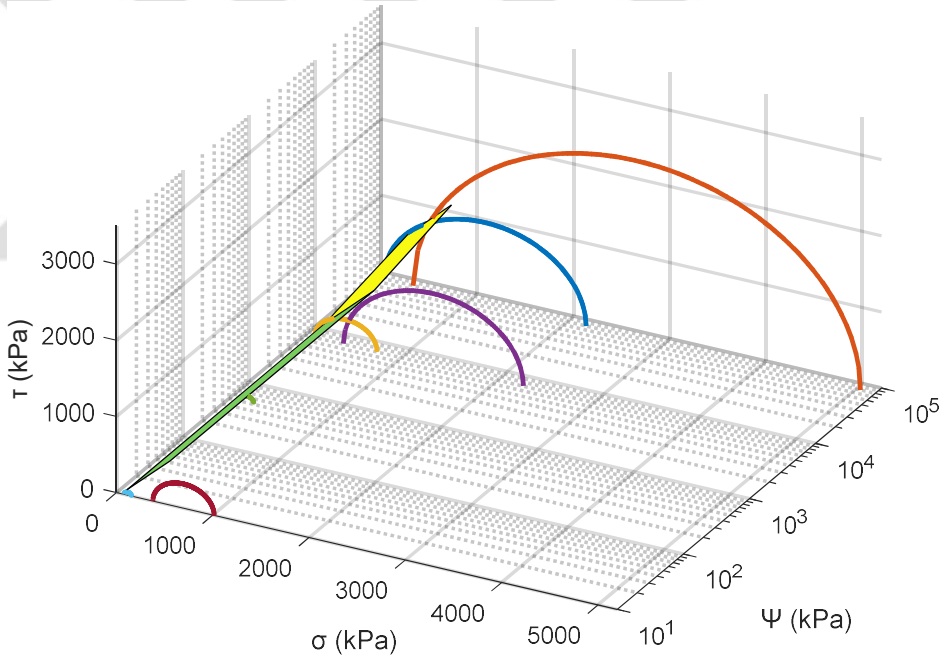

Figure 6.6. Surface plot connecting the strength envelopes obtained from the results of the best fit tangent plane in a σ-τ-ψ space

The value of effective cohesion (c’) is negative. This could be caused due to a few reasons. Firstly, as mentioned, in section 5.1.2., during the CD triaxial tests, the samples were overconsolidated 100 kPa and normally consolidated at 400 kPa. Furthermore, in the unsaturated tests, the specimens may have had some shrinkage

cracks in the middle, where they could not be seen, which would affect the shearing results.

Nevertheless, another optimization trial was carried out in which c'—and, subsequently, also a_0—were constrained as 0. Table 6.5 details the values of a_0, a_1, a_2, c', ϕ' and ϕ_b obtained from this trial.

Table 6.5 Values of parameters from optimization where c' was constrained as 0

Parameter	Value	Parameter	Value
a_0	0	c'	0
a_1	0.6911	ϕ '	43.7
a_2	0.0043	ϕ_b	0.249

Another surface plot was then plotted, this time using the results of this optimization trial where c' was kept as 0.

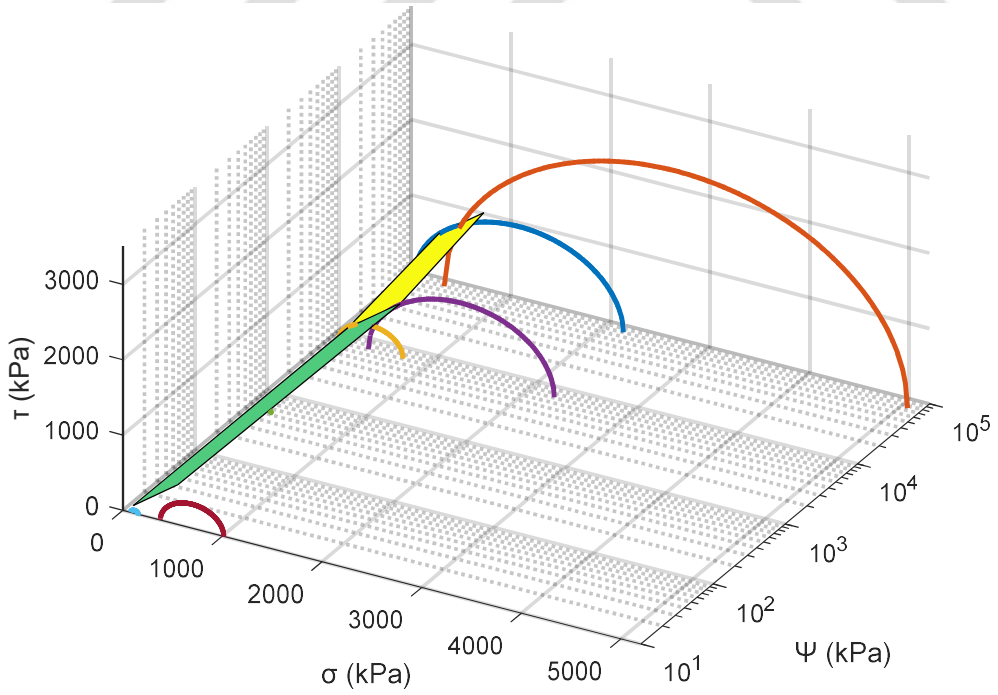

Figure 6.7. Surface plot connecting the strength envelopes obtained from the results of the second optimization trial (c' = 0) (SAME AS ABOVE)in a σ-τ-ψ space

The values of ϕ_b obtained in both optimization trials (see Tables 6.4 and 6.5) appear to be very small. However, it is important to keep in mind that the values of suction in this sample are very high. Therefore, the product of ψ and ϕ_b would have a significant enough value and, consequently, the contribution of suction to the overall shear strength would be considerable.

6.3 Comparison of Apparent Cohesion Values

Once the values of c', ϕ' and ϕ_b were obtained, a comparison was drawn in the apparent cohesion values obtained from the independent stress state approach and the effective stress state approach. The former defines the apparent cohesion as:

$$c'' = \psi tan(\phi b) \quad \text{(Eq 6.5)}$$

On the other hand, the effective stress state approach formulates apparent cohesion as:

$$c'' = \chi \psi tan(\phi') \quad \text{(Eq 6.6)}$$

where c'' is the apparent cohesion, ψ is the suction, ϕ_b is the contribution of suction to the apparent cohesion, χ is the effective stress parameter, ϕ' is the friction angle obtained from the saturated CD triaxial test.

Since multiple relationships have been defined for the effective stress parameter, a few were selected (see Table 6.6) and the apparent cohesions were calculated using them.

Table 6.6 Comparison of apparent cohesion values obtained from different equations

Suction	$\psi\tan(\varphi_b)$	Khalili & Khabbaz (1998)	Bao (1998)	Öberg and Sällfors (1997)	Vanapalli (1996)	Karube et al. (1996)
80000	316.8	29107.4	104632.2	30772.2	21194.7	8434.9
7100	28.116	3890.4	12263.3	3890.4	3890.4	2394.3
10	0.0396	5.5	28.6	5.5	5.5	5.3

As can be seen from Table 6.6, there appears to be a difference in the order of magnitude between values obtained from the two different approaches. The values of apparent cohesion from the independent stress state approach are relatively low, thereby signaling that suction does not lend a great deal of shear strength to the soil.

On the other hand, the values of apparent cohesion obtained from all of the parameters of the effective stress approach indicate that suction lends thousands of kPa of shear strength to the soil. This is in direct contradiction to the results of the triaxial experiments. Therefore, it can be concluded that none of the above selected correlations for the effective stress parameter can accurately describe the behavior of Ankara clay.

6.4 Constitutive Surface

The results of the unsaturated oedometric compression tests were plotted on an e-log σ-ψ space, as shown in Figure 6.8. Once again, the values of suction were obtained from the SWRC. Table 6.7 gives details regarding the values of suction at each moisture content.

Table 6.7 Values of suction corresponding to moisture contents of constant water content UU triaxial tests

Moisture Content (%)	Ψ (kPa)
28	630
18	11000
10	100000

Afterward, the results of the conventional oedometer (i.e. consolidation) test were also combined with the unsaturated compression tests. The saturated oedometer test was soaked throughout the duration of the tests. However, at the end of the test, when gravimetric moisture content was determined, its value came out as 25%. This can be attributed to the heterogeneity of the specimens. Therefore, even though it was soaked, it likely still experienced some level of suction. This value of suction was obtained from the fitted SWRC as 1900 kPa. Figure 6.8 depicts all four of the compression curves in an e-log σ-ψ space.

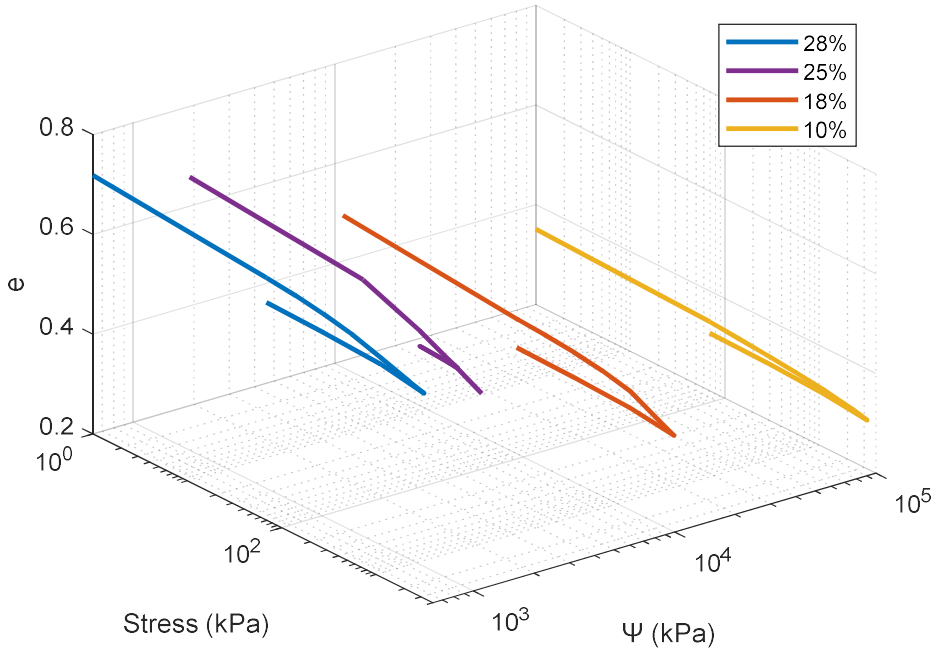

Figure 6.8. Compression curves for saturated and unsaturated oedometric compression tests in an e-log σ-ψ space

6.5 Comparison with Reconstituted Samples

As mentioned in Section 1.1 and 2.5, previous studies focused on unsaturated soil properties of Ankara clay make use of reconstituted samples and these do not accurately capture the behaviour of the soil in the field. (Kenanoğlu, 2023) carried out majority of the tests that have been carried out in this study. They conducted CD triaxial and unsaturated UU triaxials at 100 and 400 kPa confining pressures. They also determined the critical moisture content and the SWRC. Table 6.8 offers a comparison of the soil parameters obtained from their study and this study.

Table 6.8 Comparison of reconstituted and intact Ankara clay properties

Parameters	(Kenanoğlu, 2023)	Current Study
ψ_{AEV} (kPa)	2000	38000
ω_{sat} (%)	42	33
Cc	0.41	0.092
Cs	0.12	0.018
M	0.95	1.14
ϕ'	22.9°	28.37°
c' (kPa)	11.6	-16

From Table 6.8, it can be deduced that intact Ankara clay is generally denser, less compressible and has less swelling potential. Furthermore, there is a drastic difference in the ψ_{AEV} value, indicating exponentially higher values of suction.

However, it would be unwise to compare the parameters obtained from the CD triaxial tests i.e. M, φ' and c'. This is because the reconstituted samples were consolidated at 50 kPa and, hence, were normally consolidated during both tests. On the contrary, the intact samples were overconsolidated during the 100 kPa triaxial tests.

CHAPTER 7

CALIBRATION OF BARCELONA BASIC MODEL

7.1 Determination of Parameters from Experimental Results

The results of the experimental campaign were also used to calibrate the Barcelona Basic Model (BBM). The calibration procedure as outlined in (Kenanoğlu, 2023) was followed. Values of certain parameters such as κ, M, λ(0) and k were determined from the results of the saturated and unsaturated triaxial and oedometric compression tests.

As mentioned in section 5.1.2.3., the value of M was determined from the slope of the critical state line as 1.14. The value of κ was determined using the slopes of oedometric recompression lines. Firstly, the value of the friction angle was determined as 28.72, as outlined in section 5.1.2.3. This was used in conjunction with Jaky's formula to calculate the value of K_0 (Jaky, 1948):

$$K_0 = 1 - sin\phi \quad \text{(Eq 7.1)}$$

Using Eq 7.1, the value of K_0 was calculated as 0.519. The values of the slopes of the oedometric recompression lines were then converted to mean stress using the formula:

$$\kappa = C_r \log\left(\frac{1+2K_0}{3}\right) \quad \text{(Eq 7.2)}$$

where C_r is the slope of the recompression lines. Finally, the average of all values of κ was calculated as 0.0012.

λ(0) is simply the slope of the saturated virgin compression line which was determined in section 5.1.1 as 0.092. k parameter is used to quantify the contribution

of suction to the cohesion. To calculate this, the experimental values of apparent cohesion were determined from all of the UU triaxial tests as follows:

$$c = \frac{\frac{\sigma_{dev}}{2}(1-sin\,\phi)-\sigma_c sin\phi}{cos\phi} \quad \text{(Eq 7.3)}$$

where c is the total cohesion, σ_{dev} is the deviator stress, σ_c is the confining pressure and ϕ is the friction angle.

The contribution of soil suction to the cohesion i.e. the apparent tensile strength (ATS) is described as a product of the k parameter and suction and can mathematically be expressed as:

$$ATS = k * s = \frac{c''}{\tan(\phi)} \quad \text{(Eq 7.4)}$$

Therefore, the value of k can be calculated by plotting a linear relationship between p_s and suction as shown below:

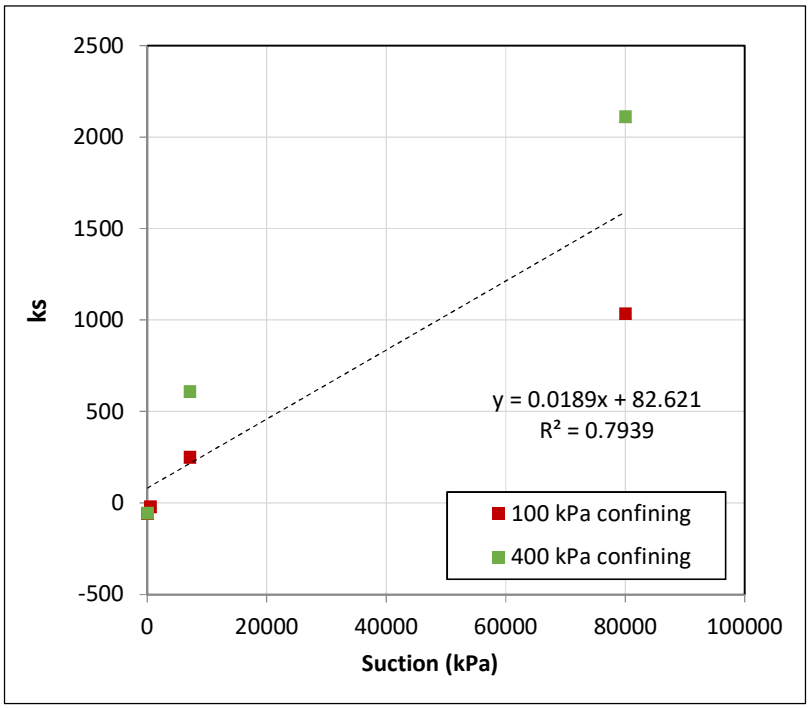

Figure 7.1. Linear relationship between ATS and suction

As can be seen in Figure 7.1, the value of k was determined as 0.0189. The value of r was determined as:

$$r = \frac{C_{r_{s\to\infty}}}{C_{r_{sat}}} \quad \text{(Eq 7.5)}$$

where $C_{r_{s\to\infty}}$ is the slope of the recompression line at the highest suction and $C_{r_{sat}}$ is its saturated counterpart.

For the value of shear modulus (G), individual values were calculated from the stress-strain graphs of all of the CD and UU triaxial results. For the calibration of UU triaxial tests, average value of all calculated G values was taken which came out as 25 MPa. However, for the calibration of oedometric compression tests, an average of G values was taken for each moisture content separately (see Table 7.1).

Table 7.1 Values of shear modulus at different moisture contents

Test	Moisture Content (%)	Average Value of G (MPa)
UU Triaxial	9-19-29	25
	28	5
Oedometer	18	15
	10	50

Values of a, n, m, θ_{sat} and θ_{res} were determined in Section 6.1 and kept the same in this calibration. Table 7.2 details the parameters and their values which were calculated from the results of the experiments

These calculated values, when input into the calibration formulations of UU triaxial tests, produced a good fit. However, for the calibration of the oedometer tests, values of certain parameters such as λ(0), κ, r, M and k had to modified to be produce a good fit. The initial calculated values of all these parameters was done from the results of the saturated and unsaturated oedometric compression tests. However, those calculated values, when input into the BBM formulations, did not accurately

model the soil behaviour. Therefore, they were changed in order to produce a good fit.

Furthermore, during the calibration procedure, values of certain parameters were manually adjusted such that the results of the model matched those of the experiments as closely as possible and errors were minimized. These included:

- p_c, which represents the stress point where plastic deformations commence
- p_0^*, which represents the initial reference stress and defines the initial position of the yield surface. This value is individually adjusted for each test since initial conditions (suction and confining pressure) were different in each
- β, which controls the rate of increase in stiffness in virgin states with suction

Table 7.2 Values of calculated parameters for UU triaxial and oedometer tests

Parameter	Value for UU triaxial tests	Value for oedometer tests
κ	0.001	0.009
r	0.422	0.570
M	1.140	1.100
$\lambda(0)$	0.092	0.020
k	0.019	0.001
a	38000	38000
n	0.550	0.550
m	1.050	1.050
θ_{sat}	0.456	0.456
θ_{res}	0.047	0.047

7.2 Results of Calibration

Finally, optimization was done and results of the BBM calibration were plotted alongside experimental results (see Figures 7.2 and 7.3).

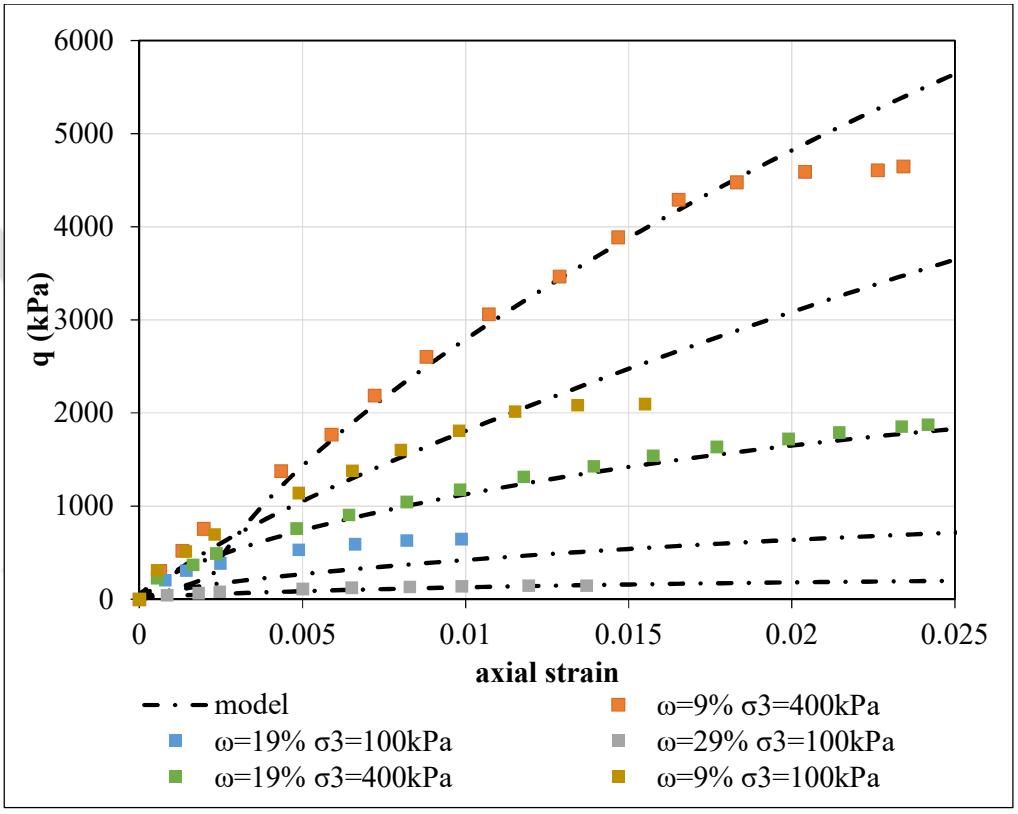

Figure 7.2. Results of calibration for UU triaxial tests

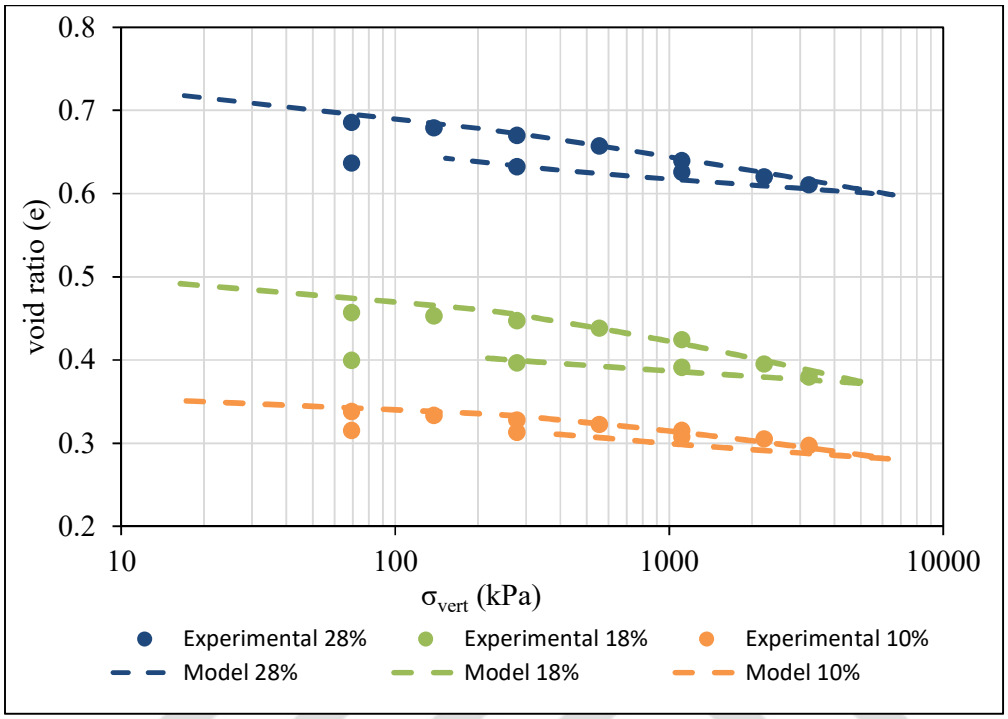

Figure 7.3. Results of calibration for oedometric compression tests

As can be seen in Figure 7.2, the results of the BBM calibration are better equipped to model low to moderate strains and do not accurately capture the behavior once yielding occurs. It is also noteworthy that this deviation appears to be more prominent in soils with higher suction. This signifies that BBM cannot accurately capture the brittle behaviour that Ankara clay exhibits at high suctions.

From Figure 7.3, it appears that the BBM is a good fit for modelling 1-D compression. However, it is important to note here that the values of input parameters were different for the UU triaxial and the oedometer tests for the same soil sample. Therefore, we conclude that BBM cannot accurately model the compressive behaviour of Ankara clay.

From the results of this calibration excercise, it can be concluded that BBM is not an apropriate model for stiff high-plasticity clays like Ankara. The main reason for this is that it cannot acurately capture the brittle behaviour that Ankara clay exhibits at high suctions. However, it is also important to note here that, Ankara clay is not

likely to experience, in the field, suctions high enough to induce this brittle behaviour. In Fıgure 7.2, it can be seen that the brittle behaviour is exhibited at 9% moisture content which corresponds to a suction of 80000 kPa. Keeping in mind that, it is unlikely that local soils in the region will experience these levels of suction.

Nevertheless, a good soil constitutive model should, in theory, be able to accurately emulate the behaviour of soil under all kinds of loadings at all moisture contents. Keeping this in mind, along with results of the calibration excercise, it can be concluded that BBM is not an apropriate model for stiff clays like Ankara clay.

CHAPTER 8

CONCLUSIONS

8.1 Conclusions

This study deals with the experimental determination of the unsaturated properties of Ankara clay in its in-situ state. For this purpose, undisturbed samples were extracted and a variety of tests were conducted on them in order to deduce their hydraulic and mechanical properties.

The results of the tests have been used to infer important properties regarding the behavior of Ankara clay, in saturated and unsaturated states. Table 8.1 highlights the values of the key properties of the METU sample obtained in this study.

Table 8.1 Soil properties of the METU sample

Soil Property	Value
Air entry value	38000 kPa
Pre-consolidation pressure (p_c)	200 kPa
Compression index (C_c)	0.092
Swelling index (C_s)	0.018
Effective cohesion (c')	-18.25 kPa
Effective friction angle (ϕ')	28.72°
Slope of critical state line (M)	1.14
Residual suction (ψ_{res})	900000
Residual volumetric moisture content (θ_{res})	10.3%
Unsaturated cohesion (c')	-57.8 kPa
Unsaturated friction angle (ϕ')	48.9
Matric suction contribution ($\phi_{b)}$	0.227

The results of this study shed light on the importance of testing soil in its in-situ state. Previous studies conducted on Ankara Clay using reconstituted samples discovered vastly different results. In its in-situ state, the soil proved to be a lot denser and more overconsolidated than anticipated. This leads to a smaller void ratio which, in turn, leads to unprecedented levels of suction in the sample. This is evident from the fact that the samples from METU had an AEV of 38 MPa.

Additionally, high amounts of suction in the soil sample also considerably alter its soil properties. As can be seen in Section 5.2.2., the friction angle of the specimen increases considerably with an increase in suction. This was a phenomenon not previously observed in studies with reconstituted samples, most likely because those samples did not experience an increase in suctions of similar magnitude.

High amounts of suction contribute to the overall strength of the soil, making it stiffer and more brittle. This makes the soil difficult to work with in a laboratory setting as cutting specimens from brittle soil leads to breakage and wastaging of specimens. This was seen in particular in the first sample from Bahçelievler, due to low natural moisture content. The samples were so stiff and brittle that they proved to be unworkable. Specimens for triaxial tests could not be extruded as they kept breaking. Therefore, the complete experimental program could not be carried out on that sample batch.

Moreover, high amounts of suction lead to difficulty in saturating the soil. The triaxial setup used in this study was not capable of applying large enough values of back-pressure saturation. Hence, a water bath had to be developed for saturating the specimens and eliminating suction entirely.

Furthermore, suction controlled tests, on this soil in an unsaturated state are not usually possible as imposing such high amounts of suction requires sophisticated techniques. Therefore, constant water content tests had to be carried out. However, at low values of suction, constant suction tests are definitely possible and should be preferred.

For constant water content tests, specimen preparation was carried out in two ways. The specimens for triaxial tests were first cut and then dried whereas, for oedometric compression tests, they were first dried and then cut. It was discovered that the former method is more preferable than the latter one as cutting of dried specimens is difficult and can result in breakage. Additionally, using sharper cutters makes the process of cutting specimens considerably easier.

Furthermore, during drying, avoiding shrinkage cracks was difficult. To overcome this, specimens should be equilibriated using vapor equilibrium technique as opposed to the air-drying method undertaken in this study. While the equilibriation time might be longer, the specimens will dry more evenly and be subjected to less shrinkage cracks.

Another way to avoid shrinkage cracks is to conduct constant water content tests at moisture contents which are closer to either the in-situ water content or the shrinkage limit. These two scenarios lead to practically no shrinkage cracks in the specimens. Specimens at intermediate water contents tend to have more shrinkage cracks (even after equilibriation) which leads to errenous results.

Finally, the Barcelona Basic Model (BBM) was calibrated using the results of the experimental campaign. The results of the calibration show that BBM cannot accurately capture and emulate the brittle behaviour that Ankara clay exhibits at high suctions. Furthermore, it does not appear to be able to accurately capture the behaviour of Ankara clay under compressive loading. In light of this, it can be concluded that BBM is not suitable for modelling the behaviour of stiff clays.

8.2 Recommendations for Future Studies

- When extracting samples from the field, it is preferrable to do it in humid weather. For the case of Ankara, that would be during the winter. This would lead to relatively less suction in the specimens in their in-situ state which, in turn, would lead to specimens being easier to cut. However, suction levels

would still be high enough to neccesiate a water bath for full saturation prior to saturated triaxial tests.

- For vapor equilibrium, more salts should be incorporated that can measure suctions higher than 90 MPa such as LiBr and $MgCl_2$ (Gao & Sun, 2017). This might allow the tail end of the retention curve to be captured.
- Triaxial tests (both saturated and unsaturated) should be carried out at confing pressures higher than the pre-consolidation pressure. This is because the behaviour of over-consolidated and normally consolidated clays tends to differ.
- In saturated and unsaturated tests, the same type of triaxial tests (e.g. CD or CU) should be carried out in saturated and unsaturated states. This will allow for a better comparison and analysis of how much strength the suction lends to the soil.
- Saturated and unsaturated triaxial tests should be carried out at the same void ratio in order to eliminate the effect of decreasing void ratio on the friction angle. This will allow for a better comparison of saturated and unsaturated strength parameters.
- For consolidation test, simply soaking the specimen is not enough to completely eliminate suction, as is evidenced in this study. Therefore, consolidation specimens should also be wetted in a water bath (similar to the triaxial specimens) prior to starting the test. However, care should be taken when transferring specimen from water bath to the test setup as sample will likely swell when removed from the water bath.
- A mechanism for measuring volume change during UU triaxials should be developed that is incorporated into the triaxial setup, rather than relying on image processing.
- For unsaturated oedometeric compression tests, a more sophistcated setup should be developed which can apply higher loads so that loading might surpass suction in the specimen.

- A retaining ring for oedometric compression tests may also be developed such that it is capable of having varying diameter (perhaps with the help of a tightening screw). This is because it is not always possible to accurately predict the diameter reduction due to drying. If the specimen does not dry to exactly the size of the retaining ring, K_0 condition cannot be ensured.
- Studies should be undertaken to develop an effective stress parameter specifically for high-plasticity, expansive clays. This can be done by gathering available literature on such soils and carrying out regression analyses. However, given the limited amount of literature available, it is likely that further testing will be necessiated.
- The results of the BBM calibration should be validated using further experiments carried out on intact samples with identical properties
- Constitutive models other than BBM should be explored for emulating the behaviour of Ankara clay
- It may also be prudent to explore constitutive models not designed specifically for unsaturated soils but still geared towards stiff high-plasticity clays such as (Hong et al., 2016); (Whittle & Kavvadas, 1994). If these models are a good fit for Ankara clay in its saturated state, they may be extended to develop formulations for the unsaturated states.

REFERENCES

A. M. Marinho, F., Gonzalo Carnero Guzmán, G., & Del Gaudio Orlando, P. (2016). Constant Water Content Compression Tests on Unsaturated Compacted Soil with Suction Measurement Using a HCT. *International Journal of Geomechanics*, *16*(6), D4015008. https://doi.org/10.1061/(ASCE)GM.1943-5622.0000609

Ahmadi Naghadeh, R. (2016). *Hydro-mechanical Behaviour of Unsaturated Isotropically Reconstituted Specimens from Slurry and Compacted Specimens*. Middle East Technical University.

Ahmadi Naghadeh, R., Toker, N. K., & Ahmadiadli, M. (2013). *Water content controlled instead of suction controlled tests*.

Aitchison, G. (1965). Soil Properties—Shear Strength and Consolidation. *Proceeding 6th Interational Conference Soil Mechanic Foundations Engineering*.

Akbas, S. O., & Kulhawy, F. H. (2010). Characterization and Estimation of Geotechnical Variability in Ankara Clay: A Case History. *Geotechnical and Geological Engineering*, *28*(5), 619–631. https://doi.org/10.1007/s10706-010-9320-x

Akgün, H., Türkmenoğlu, A. G., Met, İ., Yal, G. P., & Koçkar, M. K. (2017). The use of Ankara Clay as a compacted clay liner for landfill sites. *Clay Minerals*, *52*(3), 391–412. https://doi.org/10.1180/claymin.2017.052.3.08

Alonso, E. E., Gens, A., & Josa, A. (1990). A constitutive model for partially saturated soils. *Géotechnique*, *40*(3), 405–430. https://doi.org/10.1680/geot.1990.40.3.405

Alonso, E. E., Pereira, J.-M., Vaunat, J., & Olivella, S. (2010). A microstructurally-based effective stress for unsaturated soils. *Geotechnique*, *60*(12), 913–925. https://doi.org/10.1680/geot.8.P.002

Alonso, E. E., Vaunat, J., & Gens, A. (1999). Modelling the mechanical behaviour of expansive clays. *Engineering Geology*, *54*(1–2), 173–183. https://doi.org/10.1016/S0013-7952(99)00079-4

ASTM. (2015). *Test Methods for Pore Water Extraction and Determination of the Soluble Salt Content of Soils by Refractometer*. ASTM International. https://doi.org/10.1520/D4542-22

Aubeny, C. (2002). *Properties of High-Plasticity Clays*.

Avsar, E., Ulusay, R., & Sonmez, H. (2009). Assessments of swelling anisotropy of Ankara clay. *Engineering Geology*, *105*(1–2), 24–31. https://doi.org/10.1016/j.enggeo.2008.12.012

Benatti, J. C. B., Rodrigues, R. A., & Miguel, M. G. (2013). Aspects of Mechanical Behavior and Modeling of a Tropical Unsaturated Soil. *Geotechnical and Geological Engineering*, *31*(5), 1569–1585. https://doi.org/10.1007/s10706-013-9682-y

Bishop, A. W., & Henkel, D. J. (1964). *The Measurement of Soil Properties in the Triaxial Test*. Edward Arnold.

Blatz, J. A., Cui, Y. J., & Oldecop, L. (2009). Vapour equilibrium and osmotic technique for suction control. In *Laboratory and field testing of unsaturated soils* (pp. 49–61).

Borja, R. I. (2004). Cam-Clay plasticity. Part V: A mathematical framework for three-phase deformation and strain localization analyses of partially saturated porous media. *Computer Methods in Applied Mechanics and Engineering*, *193*(48), 5301–5338. https://doi.org/10.1016/j.cma.2003.12.067

Brooks, R., & Corey, A. (1965). Hydraulic Properties of Porous Media. *Colorado State University*.

Bulut, R., & Leong, E. C. (2008). Indirect Measurement of Suction. *Geotechnical and Geological Engineering*, *26*(6), 633–644. https://doi.org/10.1007/s10706-008-9197-0

Caicedo, B., & Thorel, L. (2014). Centrifuge modelling of unsaturated soils. *Journal of Geo-Engineering Sciences*, *2*(1–2), 83–103. https://doi.org/10.3233/JGS-130013

Chen, B., Gao, Y., Sun, D., & Li, J. (2021). Simple Testing Method for Measuring the Triaxial Stress-Strain Relations of Unsaturated Soils at High Suctions. *Geotechnical Testing Journal*, *44*(2), 535–546. https://doi.org/10.1520/GTJ20190278

Chiu, C.-K., & Ng, C. W. W. (2003). A state-dependent elasto-plastic model for saturated and unsaturated soils. *Geotechnique*, *53*, 809–829. https://doi.org/10.1680/geot.53.9.809.37426

Cokca, E., Erol, O., & Armangil, F. (2004). Effects of compaction moisture content on the shear strength of an unsaturated clay. *Geotechnical and Geological Engineering*, *22*(2), 285–297. https://doi.org/10.1023/B:GEGE.0000018349.40866.3e

Çokça, E., & Tilgen, H. P. (2010). Shear strength-suction relationship of compacted Ankara clay. *Applied Clay Science*, *49*(4), 400–404. https://doi.org/10.1016/j.clay.2009.08.028

Cui, Y., & Delage, P. (1996). Yielding and plastic behaviour of an unsaturated compacted silt. *Geotechnique*, *46*, 291–311. https://doi.org/10.1680/geot.1996.46.2.291

Delage, P., Romero, E., & Tarantino, A. (2008). *Recent developments in the techniques of controlling and measuring suction in unsaturated soils*.

Dìaz-Rodrìguez, J. A. (1992). Yielding of Mexico City Clay and Other Natural Clays. *Journal of Geotechnical Engineering*.

Eberhardsteiner, J., Hofstetter, G., Meschke, G., & Mackenzie-Helnwein, P. (2003). Coupled material modelling and multifield structural analyses in civil engineering. *Engineering Computations*, *20*(5/6), 524–558. https://doi.org/10.1108/02644400310488754

Ehlers, W., Graf, T., & Ammann, M. (2004). Deformation and localization analysis of partially saturated soil. *Computer Methods in Applied Mechanics and Engineering*, *193*(27), 2885–2910. https://doi.org/10.1016/j.cma.2003.09.026

Erguler, Z. A., & Ulusay, R. (2003). A simple test and predictive models for assessing swell potential of Ankara (Turkey) Clay. *Engineering Geology*, *67*(3–4), 331–352. https://doi.org/10.1016/S0013-7952(02)00205-3

Fredlund, D. G., & Morgenstern, N. R. (1977). Stress State Variables for Unsaturated Soils. *Journal of the Geotechnical Engineering Division*, *103*(5), 447–466. https://doi.org/10.1061/AJGEB6.0000423

Fredlund, D. G., Rahardjo, H., & Fredlund, M. D. (2012). *Unsaturated Soil Mechanics in Engineering Practice*.

Fredlund, D. G., & Xing, A. (1994). Equations for the soil-water characteristic curve. *Canadian Geotechnical Journal*, *31*(4), 521–532. https://doi.org/10.1139/t94-061

Fredlund, M., Wilson, G. W., & Fredlund, D. (2002). *Representation and estimation of the shrinkage curve*. *1*, 145–149.

Gallipoli, D., D'Onza, F., & Wheeler, S. J. (2010). A sequential method for selecting parameter values in the Barcelona basic model. *Canadian Geotechnical Journal*, *47*(11), 1175–1186. https://doi.org/10.1139/T10-017

Gao, Y., & Sun, D. (2017). Soil-water retention behavior of compacted soil with different densities over a wide suction range and its prediction. *Computers and Geotechnics*, *91*, 17–26. https://doi.org/10.1016/j.compgeo.2017.06.016

Gens, A., & Alonso, E. E. (1992). A framework for the behavior of unsaturated expansive clays. *Canadian Geotechnical Journal*, 1013–1032.

Greenspan, L. (1977). Humidity fixed points of binary saturated aqueous solutions. *Journal of Research of the National Bureau of Standards Section A: Physics and Chemistry*, *81A*(1), 89. https://doi.org/10.6028/jres.081A.011

Holtz, W. G., & Gibbs, H. J. (1954). Engineering Properties of Expansive Clays. *Transactions of the American Society of Civil Engineers*.

Hong, P. Y., Pereira, J. M., Tang, A. M., & Cui, Y. J. (2016). A two-surface plasticity model for stiff clay. *Acta Geotechnica*, *11*(4), 871–885. https://doi.org/10.1007/s11440-015-0401-0

Jaky, J. (1948). Pressure in silos. *Proc. 2nd Int. Conf. Soil Mech*, *1*.

Kenanoğlu, M. B. (2023). *Determination of Unsaturated Soil Properties from Simplified Experimental Procedures*. Middle East Technical University.

Kenanoğlu, M. B., & Toker, N. K. (2023). Microstructure-based estimation of unsaturated shear strength from simple evaporation test. *Bulletin of Engineering Geology and the Environment*, *82*(8), 315. https://doi.org/10.1007/s10064-023-03340-y

Khalili, N., Geiser, F., & Blight, G. E. (2004). Effective Stress in Unsaturated Soils: Review with New Evidence. *International Journal of Geomechanics*, *4*(2), 115–126. https://doi.org/10.1061/(ASCE)1532-3641(2004)4:2(115)

Khalili, N., & Khabbaz, M. H. (1998). A unique relationship for χ for the determination of the shear strength of unsaturated soils. *Géotechnique*, *48*(5), 681–687. https://doi.org/10.1680/geot.1998.48.5.681

Khalili, N., & Loret, B. (2001). An elasto-plastic model for non-isothermal analysis of flow and deformation in unsaturated porous media: Formulation. *International Journal of Solids and Structures*, *38*(46), 8305–8330. https://doi.org/10.1016/S0020-7683(01)00081-6

Khallili, N., Romero, E., & A. M. Marinho, F. (2022). *Proceedings of the 20th ICSMGE-State of the Art and Invited Lectures*.

Knight, R. J., Tercier, P., & Georgi, D. T. (1995, June). *A Laboratory Procedure For Estimating Irreducible Water Saturation From Cuttings*. SPWLA 36th Annual Logging Symposium, Paris, France.

Kochmanová, N., & Tanaka, H. (2011). Influence of the Soil Fabric on the Mechanical Properties of Unsaturated Clays. *Soils and Foundations*, *51*(2), 275–286. https://doi.org/10.3208/sandf.51.275

Kohgo, Y., Nakano, M., & Miyazaki, T. (1993). Theoretical Aspects of Constitutive Modelling For Unsaturated Soils. *Soils and Foundations*, *33*(4), 49–63. https://doi.org/10.3208/sandf1972.33.4_49

Leech, C., Lockington, D., & Hooton, R. D. (2006). Estimation of Water Retention Curve from Mercury Intrusion Porosimetry and van Genuchten Model. *ACI Structural Journal*, *103*(2). https://doi.org/10.14359/15187

Leong, E.-C., Tripathy, S., & Rahardjo, H. (2003). Total suction measurement of unsaturated soils with a device using the chilled-mirror dew-point technique. *Géotechnique*, *53*(2), 173–182. https://doi.org/10.1680/geot.2003.53.2.173

Li, L., & Zhang, X. (2015). A New Triaxial Testing System for Unsaturated Soil Characterization. *Geotechnical Testing Journal*, *38*(6), 823–839. https://doi.org/10.1520/GTJ20140201

Loret, B., & Khalili, N. (2000). A three-phase model for unsaturated soils. *International Journal for Numerical and Analytical Methods in Geomechanics*, *24*(11), 893–927. https://doi.org/10.1002/1096-9853(200009)24:11<893::AID-NAG105>3.0.CO;2-V

Lu, N. (2019). Revisiting Axis Translation for Unsaturated Soil Testing. *Journal of Geotechnical and Geoenvironmental Engineering*. https://ascelibrary.org/doi/epdf/10.1061/%28ASCE%29GT.1943-5606.0002055

Lu, N. (2020). Unsaturated Soil Mechanics: Fundamental Challenges, Breakthroughs, and Opportunities. *Journal of Geotechnical and Geoenvironmental Engineering*, *146*(5), 02520001. https://doi.org/10.1061/(ASCE)GT.1943-5606.0002233

Lu, N., Wayllace, A., Carrera, J., & Likos, W. (2006). Constant Flow Method for Concurrently Measuring Soil-Water Characteristic Curve and Hydraulic Conductivity Function. *Geotechnical Testing Journal*, *29*(3), 230–241. https://doi.org/10.1520/GTJ12637

Mašín, D., & Khalili, N. (2008). A hypoplastic model for mechanical response of unsaturated soils. *International Journal for Numerical and Analytical Methods in Geomechanics*, *32*(15), 1903–1926. https://doi.org/10.1002/nag.714

Mendes, J., Gallipoli, D., Tarantino, A., & Toll, D. (2019). On the development of an ultra-high-capacity tensiometer capable of measuring water tensions to 7 MPa. *Géotechnique*, *69*(6), 560–564. https://doi.org/10.1680/jgeot.18.T.008

Mendes, J., & Toll, D. G. (2016). Influence of Initial Water Content on the Mechanical Behavior of Unsaturated Sandy Clay Soil. *International Journal of Geomechanics*, *16*(6), D4016005. https://doi.org/10.1061/(ASCE)GM.1943-5622.0000594

Met, İ., & Akgün, H. (2015). Geotechnical evaluation of Ankara clay as a compacted clay liner. *Environmental Earth Sciences*, *74*(4), 2991–3006. https://doi.org/10.1007/s12665-015-4330-x

Met, İ., Akgün, H., & Türkmenoğlu, A. G. (2005). Environmental geological and geotechnical investigations related to the potential use of Ankara clay as a compacted landfill liner material, Turkey. *Environmental Geology*, *47*(2), 225–236. https://doi.org/10.1007/s00254-004-1147-4

Mitchell, J. K. (1976). *Fundamentals Of Soil Behavior*. John Wiley & Sons Inc. https://istasazeh-co.com/wp-content/uploads/2022/04/Fundamentals-Of-Soil-Behavior-K-Mitchel.pdf

Mun, W., & McCartney, J. S. (2015). Compression mechanisms of unsaturated clay under high stresses. *Canadian Geotechnical Journal*, *52*(12), 2099–2112. https://doi.org/10.1139/cgj-2014-0438

Ng, C. W. W., Zhou, C., & Chiu, C. F. (2020). Constitutive modelling of state-dependent behaviour of unsaturated soils: An overview. *Acta Geotechnica*, *15*(10), 2705–2725. https://doi.org/10.1007/s11440-020-01014-7

Nowamooz, H., & Masrouri, F. (2010). Influence of suction cycles on the soil fabric of compacted swelling soil. *Comptes Rendus. Géoscience*, *342*(12), 901–910. https://doi.org/10.1016/j.crte.2010.10.003

Oliveira, O. M., & Marinho, F. A. M. (2008). Suction Equilibration Time for a High Capacity Tensiometer. *Geotechnical Testing Journal*, *31*(1), 101–105. https://doi.org/10.1520/GTJ100800

Peroni, N., & Tarantino, A. (2005). Measurement of osmotic suction using the squeezing technique. In T. Schanz (Ed.), *Unsaturated Soils: Experimental Studies* (Vol. 93, pp. 159–168). Springer-Verlag. https://doi.org/10.1007/3-540-26736-0_13

Riad, B., & Zhang, X. (2022). Characterizing and Modeling the Coupled Hydro-Mechanical Cyclic Behavior of Unsaturated Soils Using Constant Water Content Oedometer and Direct Shear Tests. *Transportation Research Record*, *2676*(10), 173–193. https://doi.org/10.1177/03611981221088775

Ridley, A. M., & Burland, J. B. (1993). A new instrument for the measurement of soil moisture suction. *Géotechnique*, 321–324.

Romero, E., Gens, A., & Lloret, A. (1999). Water permeability, water retention and microstructure of unsaturated compacted Boom clay. *Engineering Geology*, *54*(1–2), 117–127. https://doi.org/10.1016/S0013-7952(99)00067-8

Russell, A. r., & Khalili, N. (2006). A unified bounding surface plasticity model for unsaturated soils. *International Journal for Numerical and Analytical Methods in Geomechanics*, *30*(3), 181–212. https://doi.org/10.1002/nag.475

Sheng, D., Sloan, S. W., & Gens, A. (2004). A constitutive model for unsaturated soils: Thermomechanical and computational aspects. *Computational Mechanics*, *33*(6), 453–465. https://doi.org/10.1007/s00466-003-0545-x

Sheng, D., Sloan, S. W., Gens, A., & Smith, D. W. (2003). Finite element formulation and algorithms for unsaturated soils. Part I: Theory. *International Journal for Numerical and Analytical Methods in Geomechanics*, *27*(9), 745–765. https://doi.org/10.1002/nag.295

Shwan, B. J. (2017). THE EFFECT OF SOIL WATER RETENTION CURVE HYSTERESIS ON THE STRENGTH OF UNSATURATED SOILS. *The Journal of The University of Duhok*, *20*(1), 285–292. https://doi.org/10.26682/sjuod.2017.20.1.26

Sjoblom, K. J. (2000). *The mechanisms involved during the desaturation process of a porous matrix*. Massachusetts Institute of Technology.

Tarantino, A., & Mongiovì, L. (2001). Experimental procedures and cavitation mechanisms in tensiometer measurements. In *Unsaturated soil concepts and their application in geotechnical practice* (pp. 189–210).

Toker, N. K., Germaine, J., Sjoblom, K., & Culligan, P. (2004). A new technique for rapid measurement of continuous soil moisture characteristic curves. *Geotechnique*, *54*, 179–186. https://doi.org/10.1680/geot.54.3.179.36351

Tonoz, M. C., Ulusay, R., & Gokceoglu, C. (2004). Effects of Lime Stabilization on Engineering Properties of Expansive Ankara Clay. In R. Hack, R. Azzam, & R. Charlier (Eds.), *Engineering Geology for Infrastructure Planning in Europe: A European Perspective* (pp. 466–474). Springer. https://doi.org/10.1007/978-3-540-39918-6_53

Van Genuchten, M. Th. (1980). A closed-form equation for predicting the hydraulic conductivity of unsaturated soils. *Soil Science Society of America Journal*, 892–898.

Vanapalli, S. K., Nicotera, M. V., & Sharma, R. S. (2009). Axis translation and negative water column techniques for suction control. In *Laboratory and field testing of unsaturated soils* (pp. 33–48).

Vaunat, J., Cante, J. C., Ledesma, A., & Gens, A. (2000). A stress point algorithm for an elastoplastic model in unsaturated soils. *International Journal of Plasticity*, *16*(2), 121–141. https://doi.org/10.1016/S0749-6419(99)00033-9

Wheeler, S. J. (1996). Inclusion of specific water volume within an elasto-plastic model for unsaturated soil. *Canadian Geotechnical Journal*, *33*(1), 42–57. https://doi.org/10.1139/t96-023

Wheeler, S. J., Gallipoli, D., & Karstunen, M. (2002). Comments on use of the Barcelona Basic Model for unsaturated soils. *International Journal for Numerical and Analytical Methods in Geomechanics*, *26*(15), 1561–1571. https://doi.org/10.1002/nag.259

Wheeler, S. J., & Sivakumar, V. (1995). *An elasto-plastic critical state framework for unsaturated soil*.

Whittle, A. J., & Kavvadas, M. J. (1994). Formulation of MIT-E3 Constitutive Model for Overconsolidated Clays. *Journal of Geotechnical Engineering*, *120*(1), 173–198. https://doi.org/10.1061/(ASCE)0733-9410(1994)120:1(173)

Wijaya, M., & Leong, E. C. (2016). Performance of high-capacity tensiometer in constant water content oedometer test. *International Journal of Geo-Engineering*, *7*(1), 13. https://doi.org/10.1186/s40703-016-0027-6

Zhang, X., Lu, H., & Li, L. (2016). Use of Oedometer Equipped with High-Suction Tensiometer to Characterize Unsaturated Soils. *Transportation Research Record*, *2578*(1), 58–71. https://doi.org/10.3141/2578-07

APPENDIX: PICTURES OF LABORATORY TESTS

Figure A.1. (a) Sample extraction at the METU site, (b) samples in shelby tubes at the METU site, (c) specimen extrusion in the lab and (d) problematic specimen extruded from the Bahçelievler sample

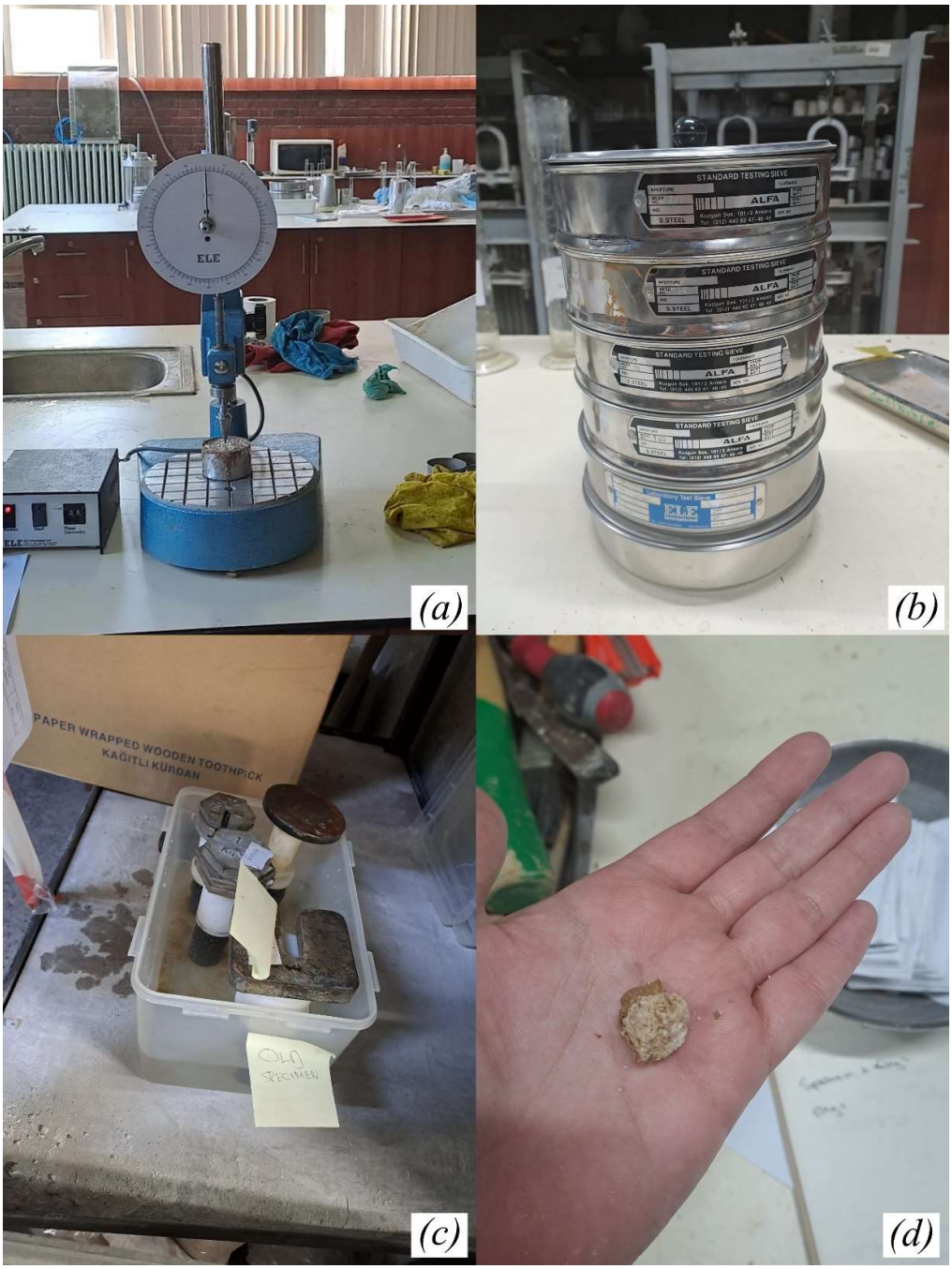

Figure A.2. (a) Fall cone test, (b) sieve set for sieve analysis, (c) water bath for saturation of triaxial specimens and (d) gravel found in one of the failed triaxial specimen extrusions

Figure A.3. Temperature chambers for vapor equilibrium: (a) refrigerator, (b) ice-box, (c) low temperature oven

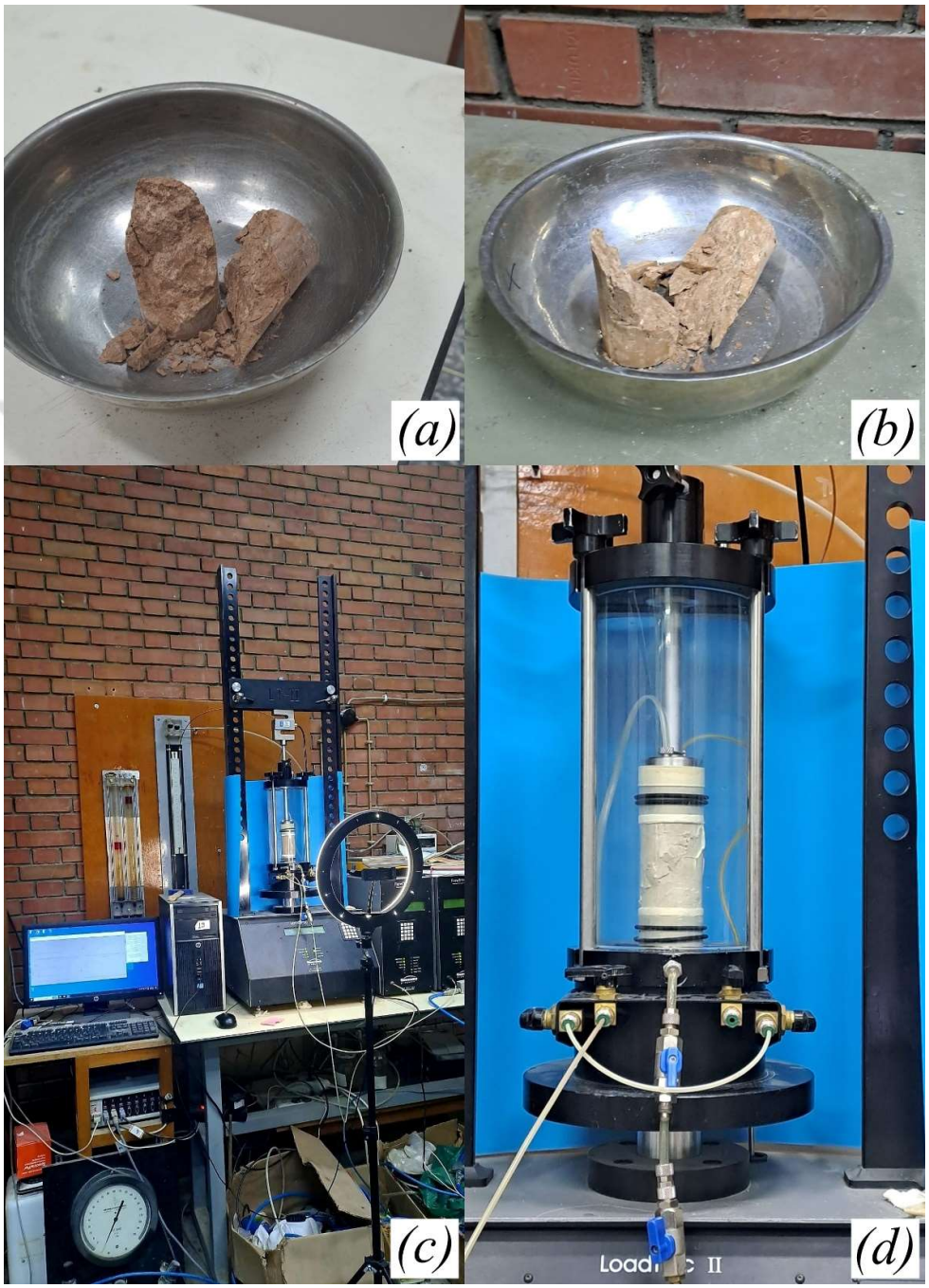

Figure A.4. (a) Specimen after failure in the 100 kPa unsaturated UU triaxial test at 9% water content, (b) Specimen after failure in the 400 kPa unsaturated UU triaxial test at 9% water content, (c) Unsaturated UU triaxial test setup and (d) Failed specimen inside the test chamber